Flood basalt structures and textures as guides to cooling histories and palaeoclimates: the Deccan Traps of Saurashtra, western India

Hetu Sheth[1] [ID], Raymond A. Duraiswami[2], Vivek Ghule[1], Anmol Naik[1] [ID] and Tarulata Das[1]

[1]Department of Earth Sciences, Indian Institute of Technology Bombay, Powai, Mumbai 400076 India and [2]Department of Geology, Savitribai Phule Pune University, Ganeshkhind, Pune 411007 India

Original Article

Abstract

The primary features (morphologies, structures, textures) of volcanic lava flows are determined by parameters such as composition, temperature, crystallinity, viscosity, flow velocity, strain rate and cooling rate. However, lava flows are open systems, and their primary features are strongly influenced by their emplacement environment. Among subaerial lava flows, those that solidify in a wet environment with rainfall develop very different internal structures (e.g. jointing patterns) and textures from those in a dry environment. Thus, the outcrop structures and textures of ancient lava flows, such as those forming continental flood basalt sequences thousands of metres thick, provide clues to their cooling histories and the palaeoclimates. Here we provide field, petrographic and geochemical data on large tholeiitic lava flows (sheet lobes) and associated dykes of the Saurashtra region in the northwestern Deccan Traps continental flood basalt province (India). The sheet lobes are dominantly pāhoehoe and rubbly pāhoehoe, and occasionally ʻaʻā, with colonnade and entablature tiers. We show that the jointing patterns in the entablatures (irregular, chevron, rosette and skeleton jointing), and the textures of the sheet lobes and even some dykes (abundant glass, and quench crystals of plagioclase and Fe–Ti oxides) reflect convective heat removal, owing to widespread interaction with meteoric waters (rainfall) during solidification. The observations thus provide evidence for a wet climate in western India 65.5 million years ago.

CAMBRIDGE
UNIVERSITY PRESS

1. Introduction

Large-scale basaltic volcanism is a major contributor to environmental stress and change. The disastrous environmental impact of the historical (1783–84), 15 km³ Laki basaltic eruption in Iceland (Guilbaud *et al.* 2005) is well known. The prehistoric continental flood basalt (CFB) provinces were constructed from large numbers of such eruptions, each of which may have produced hundreds to thousands of cubic kilometres of lava with significant volatile release over only short periods of time (years to decades, e.g. Self *et al.* 1997, 2014). It is therefore unsurprising that many CFB events correlate with biological mass extinctions (e.g. Wignall, 2001; Ernst & Youbi, 2017).

Flood basalt lava flows have been described as simple or compound (Walker, 1971). A simple lava flow is a thick and laterally extensive flow not divisible into internal units; a compound lava flow is composed of numerous individual flow-units (Nichols, 1936). Each flow-unit or lobe (Self *et al.* 1997) is a separate cooling and vesiculation unit bounded by a chilled glassy crust. Lobes range in size from toes, up to 50 cm thick and 100 cm in the long dimension, to sheet lobes that are tens of metres thick and kilometres to tens or even hundreds of kilometres long (Self *et al.* 1997; Thordarson & Self, 1998), and correspond to Walker's (1971) simple flows.

In sheet lobes that are essentially stationary due to lack of new lava supply, and are solidifying, columnar joints form due to thermal contraction of the lava (Fig. 1). By linking up laterally, and propagating downwards from the top and upwards from the base, they divide the lobe into columns with five, six or seven sides. Each column grows by small increments of brittle fracturing and crack propagation at the transition between solidified and liquid lava, as the lobe cools progressively inwards. This leaves horizontal striations on the face of a joint column (Fig. 1a), called chisel marks (James, 1920) or striations (Ryan & Sammis, 1978; DeGraff & Aydin, 1987; DeGraff *et al.* 1989). A thick sheet lobe can develop several subhorizontal tiers with distinct jointing characteristics (Fig. 1b–d). A tier characterized by a regular arrangement of relatively thick, well-formed columns is called a colonnade, whereas a tier characterized by thin (<10 cm), chaotically arranged columns is called an entablature (Tomkeieff, 1940). Whereas colonnade tiers form during slow, conductive cooling of a sheet lobe, entablature tiers reflect rapid cooling with the involvement of meteoric water (rainfall or displaced drainage) and

Fig. 1. (Colour online) (a) Exceptionally well-developed chisel marks on joint columns forming the colonnade of the Garni intracanyon lava flow, Armenia, a basaltic trachyan-desite of mid-Pleistocene age (Neill *et al.* 2015). Geologist is Davit Manucharyan. (b) Colonnade and overlying entablature in a dipping basaltic lava flow many tens of metres thick, exposed near Güvem and part of the Miocene-age Kizilçahamam volcanics near Ankara, Turkey (Kazanci, 2012). People in the foreground provide a scale. Note the much greater thickness of the entablature compared to the colonnade. (c) Colonnade and entablature in a Columbia River flood basalt lava flow tens of metres thick, in Washington, USA. Car for scale. (d) Colonnade and entablature in a 120 m thick olivine tholeiite lava flow of the Talisker Bay Group, Isle of Skye, Scotland (Williamson & Bell, 1994). People for scale. Photos by H. Sheth; the characteristically sharp boundaries between the colonnade and entablature tiers in panels (b)–(d) are indicated by the short white dashed line.

resultant steam convection within a solidifying lobe (Saemundsson, 1970; Long & Wood, 1986; Lyle, 2000; Forbes *et al.* 2014) (Fig. 1b–d).

If so, the internal structures and jointing patterns of ancient, subaerially emplaced CFB sheet lobes provide clues to the palaeo-climates. This is the aspect we explore in this study with regard to the Deccan Traps CFB province of India. We present field data on the morphologies and primary outcrop structures of tholeiitic sheet lobes and associated dykes exposed in the Saurashtra region of the northwestern Deccan Traps, along with petrographic and geochemical data. We show that these datasets together provide valuable insights into their cooling and solidification histories and thereby on the palaeoclimatic conditions during Deccan Traps CFB volcanism.

2. Volcanology of the Deccan tholeiites

The broad term tholeiite refers variably to mafic to intermediate volcanic rocks of subalkalic, silica-saturated to silica-oversaturated, and iron-rich character, and includes both basalts and basaltic andesites *sensu stricto* (Chayes, 1966). Most CFB lava flows (and associated dykes and sills), including the bulk of the Deccan Traps of India, are tholeiites that meet all these criteria (e.g. J. E. Beane, unpub. Ph.D. thesis, Washington State Univ., 1988; Sheth *et al.* 2013; Cucciniello *et al.* 2022).

The Late Cretaceous–Palaeogene (~65.5 Ma) Deccan Traps CFB province (Fig. 2) covers 500 000 km^2 in western and central India, and has been extensively studied in terms of petrology, geochemistry and geochemical stratigraphy (e.g. Krishnamurthy, 2020; Kale *et al.* 2020). Tholeiitic lava flows attain a cumulative thickness of ~2 km in the region of the Western Ghats escarpment and of ~1 km in other parts such as the Satpura Range in the northern part of the province (e.g. Bondre *et al.* 2004; Jay *et al.* 2009), though in Saurashtra and Kachchh in the northwest, maximum preserved thicknesses are a few hundred metres (Sheth *et al.* 2013). Both compound and simple flows are found in abundance (Walker, 1971; Deshmukh, 1988; Bondre *et al.* 2004; Sheth, 2018; Kale *et al.* 2022). The small-scale compound pāhoehoe flows are usually pervasively altered, contain basal pipe vesicles and are frequently hummocky, i.e. they contain tumuli
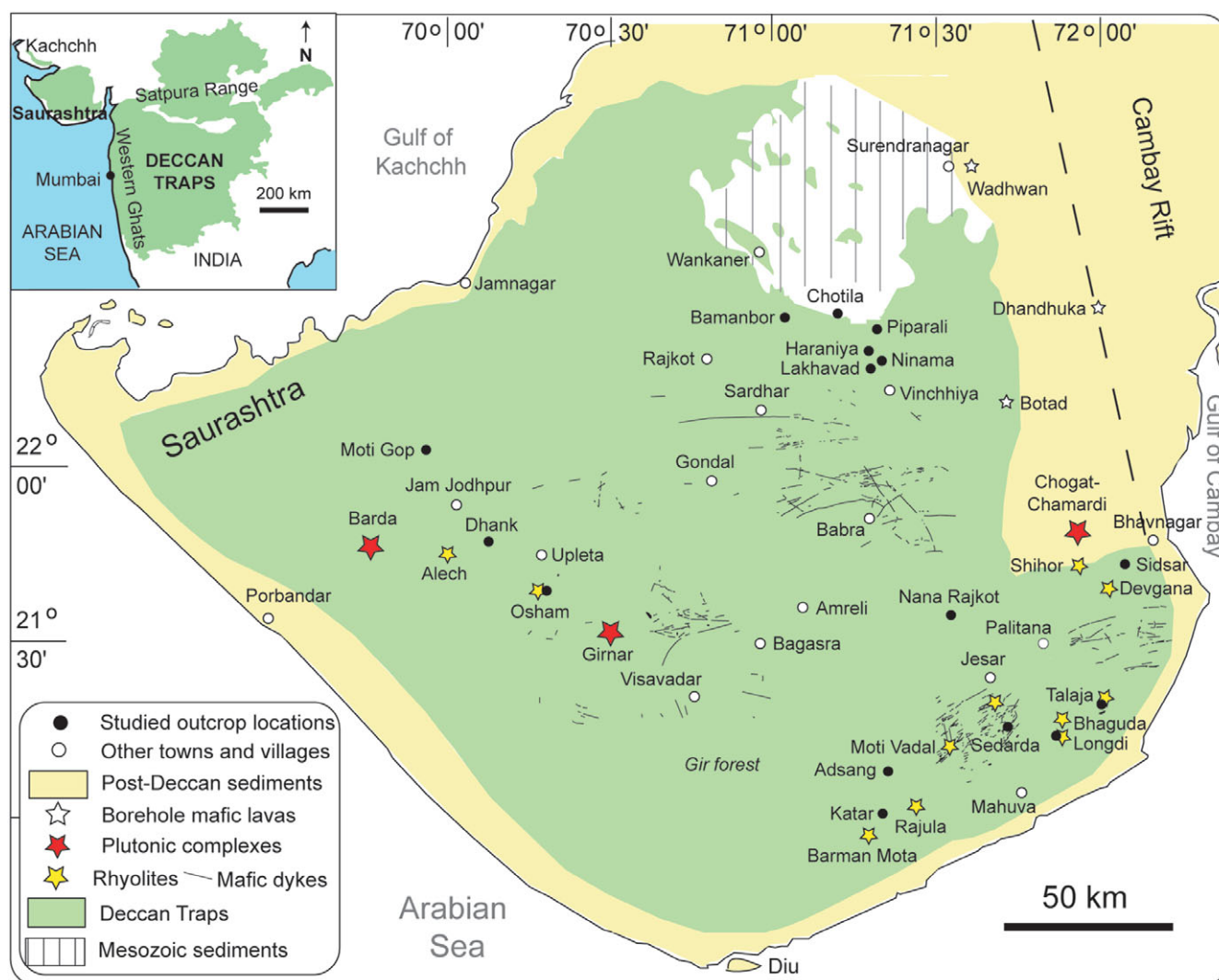
Fig. 2. (Colour online) Geological map of Saurashtra, showing the main geological features and outcrop localities mentioned in the text (filled circles). Based on Misra (1999) and Cucciniello *et al.* (2022).

(e.g. Duraiswami *et al.* 2001; Sheth *et al.* 2017*b*). The sheet lobes are of pāhoehoe and rubbly pāhoehoe, the latter with extensively brecciated upper crusts (e.g. Duraiswami *et al.* 2008; Sheth *et al.* 2017*a*; Monteiro *et al.* 2021). 'A'ā flows, characterized by both upper and basal breccias (Macdonald, 1953; Rowland & Walker, 1990; Harris *et al.* 2017), are rare in the Deccan Traps (Brown *et al.* 2011; Duraiswami *et al.* 2014), as they are in other CFB provinces such as the Columbia River province (Bondre & Hart, 2008).

3. Field observations

Almost no published information exists on the physical features of the tholeiitic lava flows of the Saurashtra (syn. Kathiawar) peninsula, such as the lava morphotypes and their primary structures including jointing patterns. Typical small-scale compound pāhoehoe flows are common and widespread across Saurashtra (Fig. 3). In this paper we focus on the sheet lobes, which are also widespread throughout the region (Figs 4–11). Whereas many are horizontally disposed, those exposed in the coastal plains of eastern and southeastern Saurashtra (Fig. 2) show significant (5–30°) structural dips as a result of post-eruptive faulting related to the

tectonic development of the Cambay rift and the western Indian rifted margin (Fedden, 1884; Misra, 1981, 1999; Ramasamy, 1995). All locations mentioned in the text are marked on Figure 2, and all GPS-derived coordinates and elevations (above mean sea level, with an uncertainty of ±3 m) are reported in online Supplementary Material Tables S1 and S2.

Near Talaja, on the road to Mahuva, two sheet lobes with a structural dip of 14° E are exposed in an abandoned quarry pit, separated by a brown bole bed (Fig. 4a, b). The upper sheet lobe (numbered SS15) shows an entablature tier above and a colonnade tier below (Fig. 4a). The entablature has a highly irregular fracture pattern. It has strongly curved fractures, vertical fractures which bound zones of subhorizontal joint columns, and metres-thick zones with hundreds of small, closely spaced subhorizontal columns exposed as polygons in vertical section (Fig. 4c, d). The colonnade, many metres thick on the north side of the quarry (Fig. 4a), thins to only ~1.5 m southwards where it overlies the brown bole (Fig. 4b–d). The quarrying has obliterated the column faces in the colonnade but its horizontal chisel marks remain well defined (Fig. 4d). The contact between the colonnade and the underlying ~2 m thick brown bole bed is planar and undisturbed
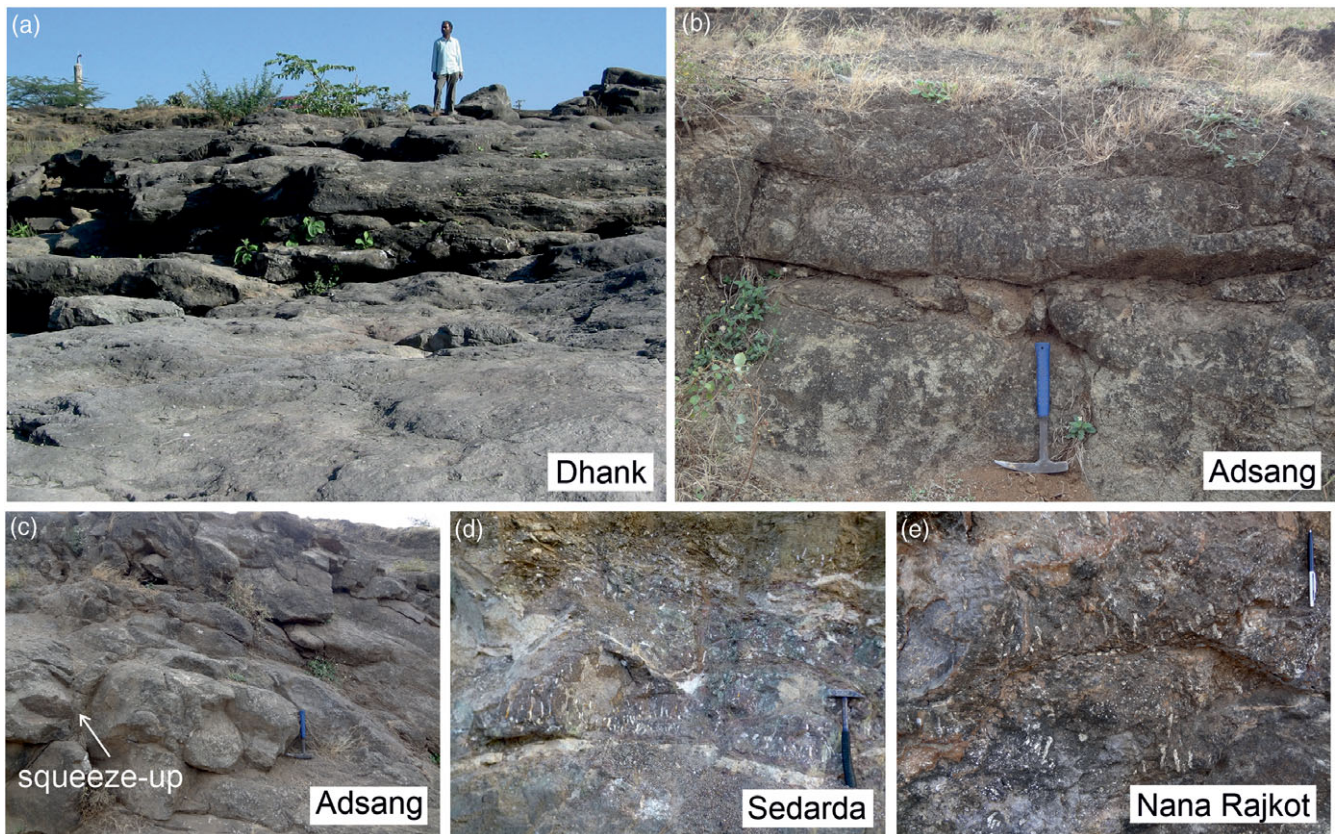
Fig. 3. (Colour online) Small-scale compound pāhoehoe lava flows in Saurashtra and their typical features (lobes and toes, squeeze-ups, pipe vesicles). The locations are marked in Figure 2. (a) Lobes and toes on the Vinu river bed 5 km east of Dhank. (b, c) Lobes and toes at Adsang. Outcrop location is 21° 07′ 06.6″ N, 71° 20′ 37.9″ E, 153 m. (d) Toes with pipe vesicles near Sedarda (21° 14′ 51.0″ N, 71° 42′ 41.8″ E, 111 m). (e) Toes with pipe vesicles at Nana Rajkot. Outcrop location is 21° 34′ 28.2″ N, 71° 33′ 00.1″ E, 130 m. All views are vertical section views; hammer for scale in (b)–(d) is 33 cm long and pen in (e) is 15 cm long. Besides these, such flows are also found, for example, at Osham Hill at 21° 37′ 53.6″ N, 70° 17′ 30.7″ E.

(Fig. 4b, d–f). Below the brown bole, flow-top breccia (the uppermost part of an underlying rubbly pāhoehoe sheet lobe), in various stages of disintegration, is exposed (Fig. 4b, e, f).

A road-cut exposure north of Longdi shows the entablature of a sheet lobe (numbered SS17) which has a structural dip of 10° E (Fig. 5a). The entablature shows sets of downward-fanning columns (chevrons), and no colonnade is exposed. A road-cut exposure near Katar shows the colonnade of a gently south-dipping sheet lobe (Fig. 5b). The colonnade shows chisel marks, and no entablature is exposed (Fig. 5c). A rock quarry at Sidsar exposes two sheet lobes with an appreciable structural dip of 30° N (Fig. 5d). The upper sheet lobe (Sid01) shows a well-formed colonnade tier tens of metres thick, with its overlying parts quarried away (Fig. 5d, e). This colonnade rests over flow-top breccia, exposed at ground level (Fig. 5f) and forming the uppermost part of an underlying rubbly pāhoehoe sheet lobe.

Ground elevations rise to 140–200 m in the north-central Saurashtra highlands around Gondal and Chotila (Fig. 2), in which we have observed numerous sheet lobes. At Lakhavad, the sides of a stream channel expose a well-formed colonnade tier of a richly plagioclase-phyric sheet lobe (BB10), with individual columns a few metres wide (Fig. 6a, b). The colonnade is overlain by massive 'intertrappean' limestone on the banks (Fig. 6c). A few kilometres to the north, well-bedded intertrappean calcareous shale and marl at Ninama (Fig. 6d, e) have been reported to contain freshwater fishes and palynoflora interpreted to be of Paleocene age (Borkar, 1973; Samant *et al.* 2014). Intertrappean beds are also

known around Bamanbor, Wankaner and Rajkot (Fedden, 1884; Borkar, 1973; Shekhawat & Sharma, 1996).

Further north of Ninama, a sheet lobe with a crudely formed colonnade (BB16) is exposed near Haraniya (Fig. 7a, b). Its relationship with the highly plagioclase-phyric Lakhavad sheet lobe BB10 (Fig. 6a, b) is unclear; both occur at comparable elevations but are distinct in petrographic characteristics. Sheet lobe BB16 is underlain by the welded flow-top breccia of a rubbly pāhoehoe sheet lobe, with centimetres-thick, laterally discontinuous black soil between the two flat-lying sheet lobes (Fig. 7b, c). A section 4.7 km north of here again exposes the same two sheet lobes. The upper sheet lobe (here numbered BB18) is a relatively well-formed colonnade, with its upper part eroded, and the lower sheet lobe is represented by flow-top breccia (Fig. 7d, e). Their contact is gently undulating on a small scale (and flat on a larger scale), and shows a laterally discontinuous black soil (Fig. 7d). The flow-top breccia is metres thick and nonwelded at this location (Fig. 7e, f).

Chotila Hill (334 m), a significant elevation in the surrounding flat landscape at ~200 m (Fig. 8a), has been described as an eroded intrusive plug (Merh, 1995). Its mostly soil-covered slopes offer few rock exposures. However, a dyke is exposed on the southern lower slopes as two en échelon segments. The first (BB04) is 90 cm thick, subvertical and strikes N 60° W (Fig. 8b). The second, southern segment (BB08) is 50 cm thick, strikes N 70° W and dips 64° due NNE (Fig. 8c). The southern upper slopes of the hill show a scar left by a debris flow, with the resulting deposit occupying lower

Fig. 4. (Colour online) Features of sheet lobes exposed 3 km southwest of Talaja on the road to Mahuva. Location of the outcrop is 21° 19′ 59.9″ N, 72° 00′ 49.4″ E, elevation 36 m. Persons provide a scale in all photographs. (a) Broad view of a sheet lobe SS15 with entablature and colonnade tiers. The lobe dips 14° E, into the plane of the photograph. (b) Lateral extension of the sheet lobe in (a), showing the entablature and colonnade, an underlying brown bole bed and a sheet lobe with flow-top breccia (FTB), thus a rubbly pāhoehoe lobe, under the bole. (c, d) Close-up views of a part of the sheet lobe SS15, showing the extremely irregular jointing and fracture patterns in the entablature, the chisel marks in the much thinner colonnade and the uppermost part of the brown bole. (e) Flow-top breccia of the rubbly pāhoehoe sheet lobe underlying the brown bole. Geologist is Alok Kumar. (f) Close-up of the highly disintegrated flow-top breccia under the bole.
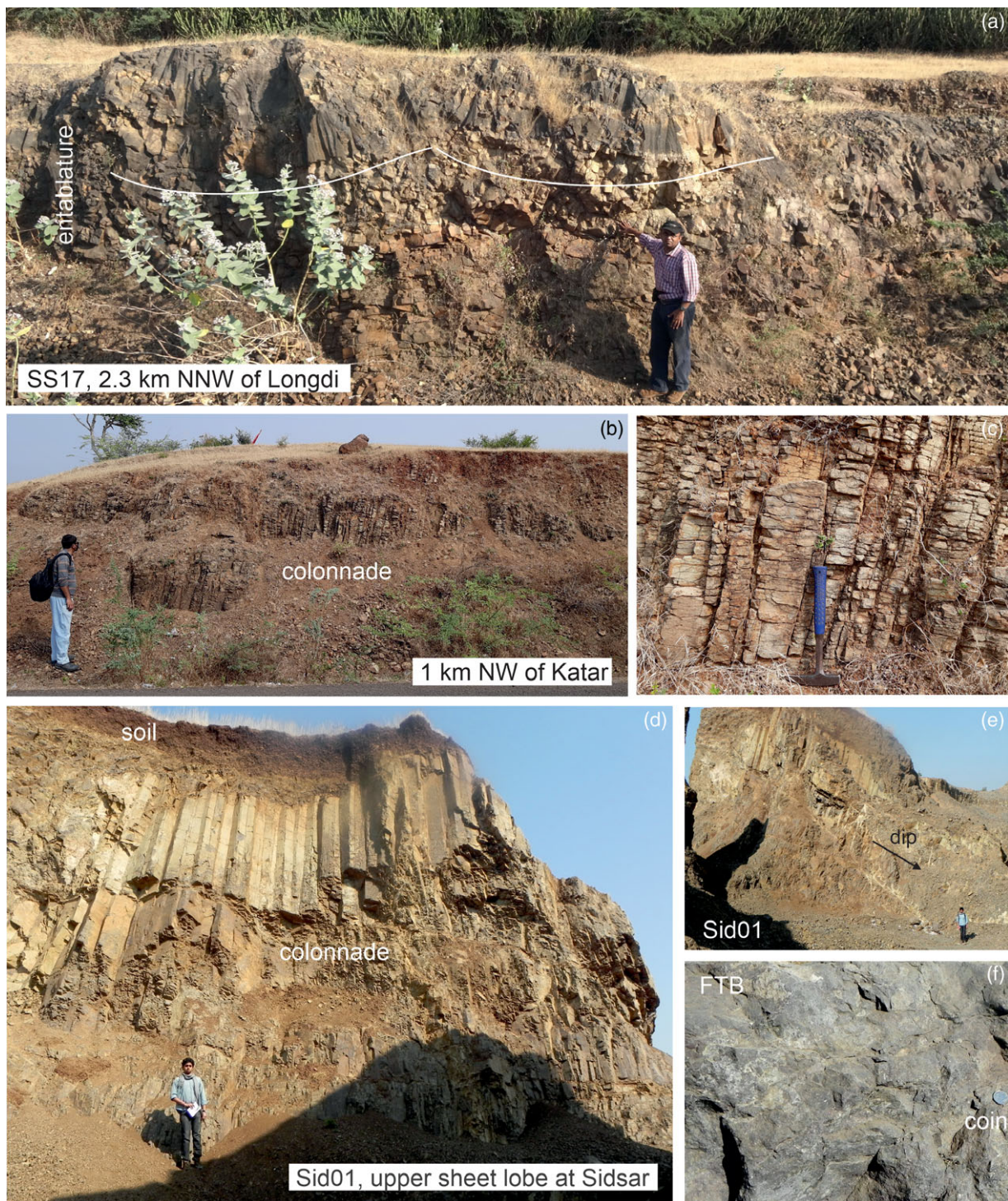
Fig. 5. (Colour online) (a) Road-cut exposure 2.3 km N 32° W of Longdi, showing chevron jointing in the entablature of the sheet lobe SS17, which dips gently away from the viewer. The interpreted cuspate shape of the isotherms during the solidification of the entablature is shown by the white line. Location is 21° 13′ 45.9″ N, 71° 52′ 32.2″ E, 56 m. (b) Road-cut exposure 1 km northwest of Katar on the Dedan road, showing a colonnade of a sheet lobe. The lobe dips gently towards the right (south). Location is 21° 00′ 26.8″ N, 71° 19′ 59.3″ E, 70 m. Geologist is Janisar M. Sheikh. (c) Detail of chisel marks on joint columns of the Katar colonnade. Vertical section; hammer for scale is 33 cm long. (d) Thick, well-formed colonnade of the upper sheet lobe of two at Sidsar (21° 43′ 7.7″ N, 72° 06′ 41.8″ E, 38 m), with a structural dip of 30° N (directly away from the viewer). Person for scale. (e) Strike-parallel view of the thick colonnade of the Sidsar upper sheet lobe, showing the structural dip. Person for scale. (f) Flow-top breccia (FTB) of the Sidsar lower sheet lobe, underlying the colonnade shown in (d) and (e). Coin for scale is 2.5 cm wide.

ground (Fig. 8d). This entirely unsorted, structureless deposit gives the false impression of volcanic breccia, and was interpreted as such by Fedden (1884, p. 21), which implies the debris flow to have formed prior to 1884. Basalt blocks in the debris flow deposit are relatively fresh (Fig. 8d), unlike the highly altered small-scale compound pāhoehoe flows of the Deccan Traps (Fig. 3). Because the debris flow deposit was derived from the hill's uppermost slopes (as attested to by the still-present scar), this implies the
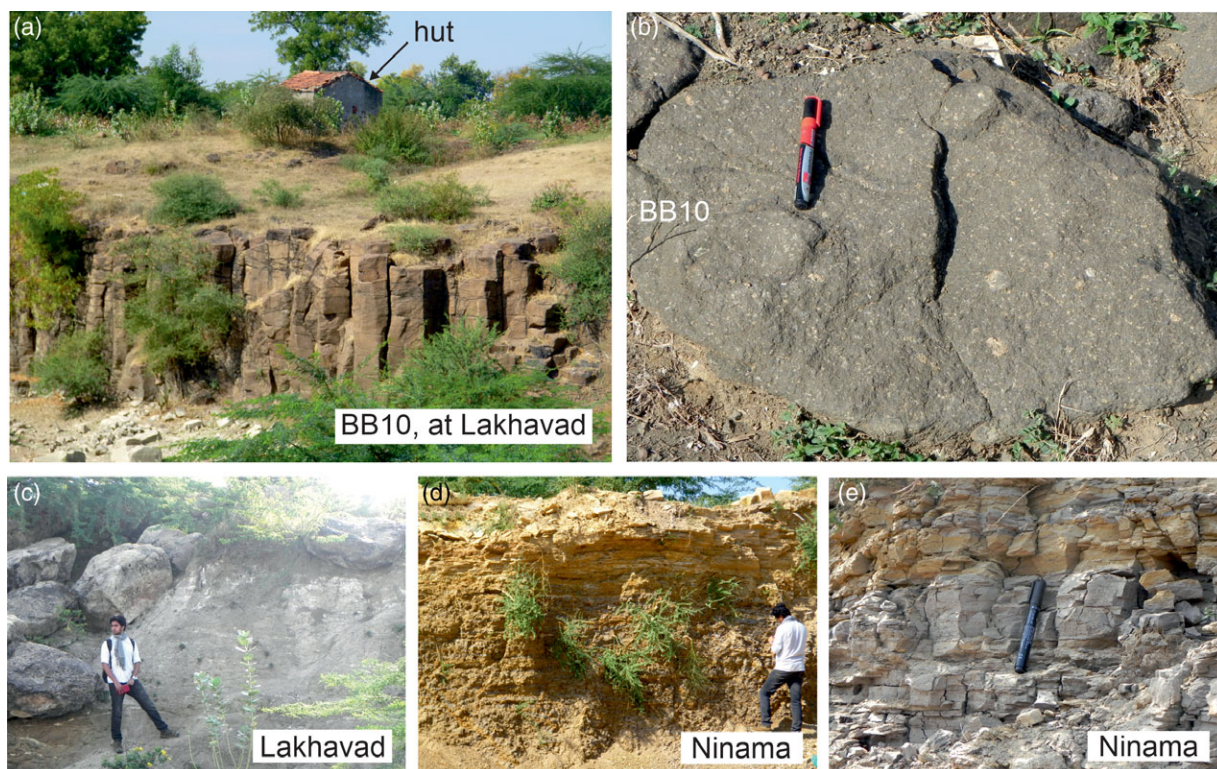
Fig. 6. (Colour online) (a) Colonnade of sheet lobe BB10 at Lakhavad (22° 14′ 27.2″ N, 71° 19′ 22.5″ E, 177 m). Hut at the back provides a scale. (b) Plan view of one of the polygonal joint columns of sheet lobe BB10. The rock is rich in small plagioclase phenocrysts. Pen for scale is 14 cm long. (c) Massive limestone bed overlying the colonnade shown in (a) and (b). (d) Well-bedded intertrappean sedimentary sequence of calcareous shale and marl, exposed outside Ninama, 5.6 km N 32° E of Lakhavad. Location is 22° 18′ 0.8″ N, 71° 21′ 07.5″ E, 148 m. (e) Close-up of the Ninama intertrappean sedimentary sequence. Vertical section, pen for scale is 14 cm long.

upper elevations of the hill to be composed of a sheet lobe. The lower elevations of the hill at ~200 m (Fig. 8a) expose an entablature of a sheet lobe (Fig. 8e). Chotila Hill is thus not an intrusive plug (cf. Merh, 1995), but a remnant of extensive erosion of the surrounding terrain composed of two or more sheet lobes.

West of Chotila, on the National Highway 8B around Bamanbor, a thick sheet lobe is exposed. The sheet lobe shows a 12 m thick entablature tier with its top eroded and base unexposed, and traversed by innumerable joint sets (Fig. 9a); sample BB03 was collected from this entablature at road level. This may be the same entablature as observed at the base of Chotila Hill (Fig. 8e). Locally the entablature shows open, centimetres-wide master joints (Fig. 9a) spaced several metres apart. When followed laterally, the road-cut exposure locally shows an upper colonnade tier (~5 m preserved thickness), composed of thin (~10 cm), well-formed, vertical columns with chisel marks (Fig. 9b). The boundary between the entablature and the upper colonnade is gently undulating, and the upper colonnade stands eroded over much of the extent of the sheet lobe which continues for several kilometres further west of Bamanbor towards Rajkot. The joint sets in the entablature range from vertical to horizontal, they splay and merge, and form radial and other (some very irregular) jointing patterns (Fig. 9b–f).

North of Bamanbor, on the road to Wankaner, a well-formed lower colonnade of the sheet lobe is exposed (Fig. 9g). It is at least ~10 m thick, making the Bamanbor sheet lobe ≥27 m thick, and sample BB01 was collected from it. Unlike the columns in the upper colonnade (Fig. 9b), individual columns in the lower

colonnade are several metres wide and display subhorizontal chisel marks (Fig. 9g, h).

The Moti Gop Hill (335 m, Fig. 10a) is composed of 16 lava flows, most of them sheet lobes, with small-scale compound pāhoehoe lava flows found at two levels (online Supplementary Material Table S2). The sheet lobes are metres in thickness (Fig. 10b), and one of them (F7) shows a lateral transition over a distance of tens of metres into small-scale, highly vesicular-amygdaloidal, compound pāhoehoe lobes and toes (Fig. 10c). Sheet lobes at the top of the section show crude subvertical columnar jointing (Fig. 10d). Sheet lobe F14 has an upper crust with spherical vesicles now filled by secondary minerals. The overlying sheet lobe F15 has pipe vesicles at the base and a core with a large number of vertical, closely spaced vesicle cylinders, filled by secondary minerals (Fig. 10e). The pipe vesicles at the base of F15 indicate that the prominent horizontal discontinuity in Figure 10e is indeed a contact between F15 and F14, and not just a horizontal fracture within a single sheet lobe.

A tholeiitic dyke (MG10) cuts the Moti Gop Hill lava flow F9 (online Supplementary Material Table S2). The dyke is 80 cm thick, strikes N–S and dips 77° due E.

The sheet lobes described so far in this paper are all pāhoehoe or rubbly pāhoehoe. Flow F10 at ~277 m elevation in the Moti Gop Hill is however an 'a'ā sheet lobe, with basal and upper breccias (Fig. 10f). The basal breccia is extensively altered to red bole-like material (Fig. 10g). An excellent example of an 'a'ā sheet lobe is exposed at Adsang (Fig. 11), where it overlies the compound pāhoehoe lobes and toes shown in Figure 3b, c. The 'a'ā sheet lobe
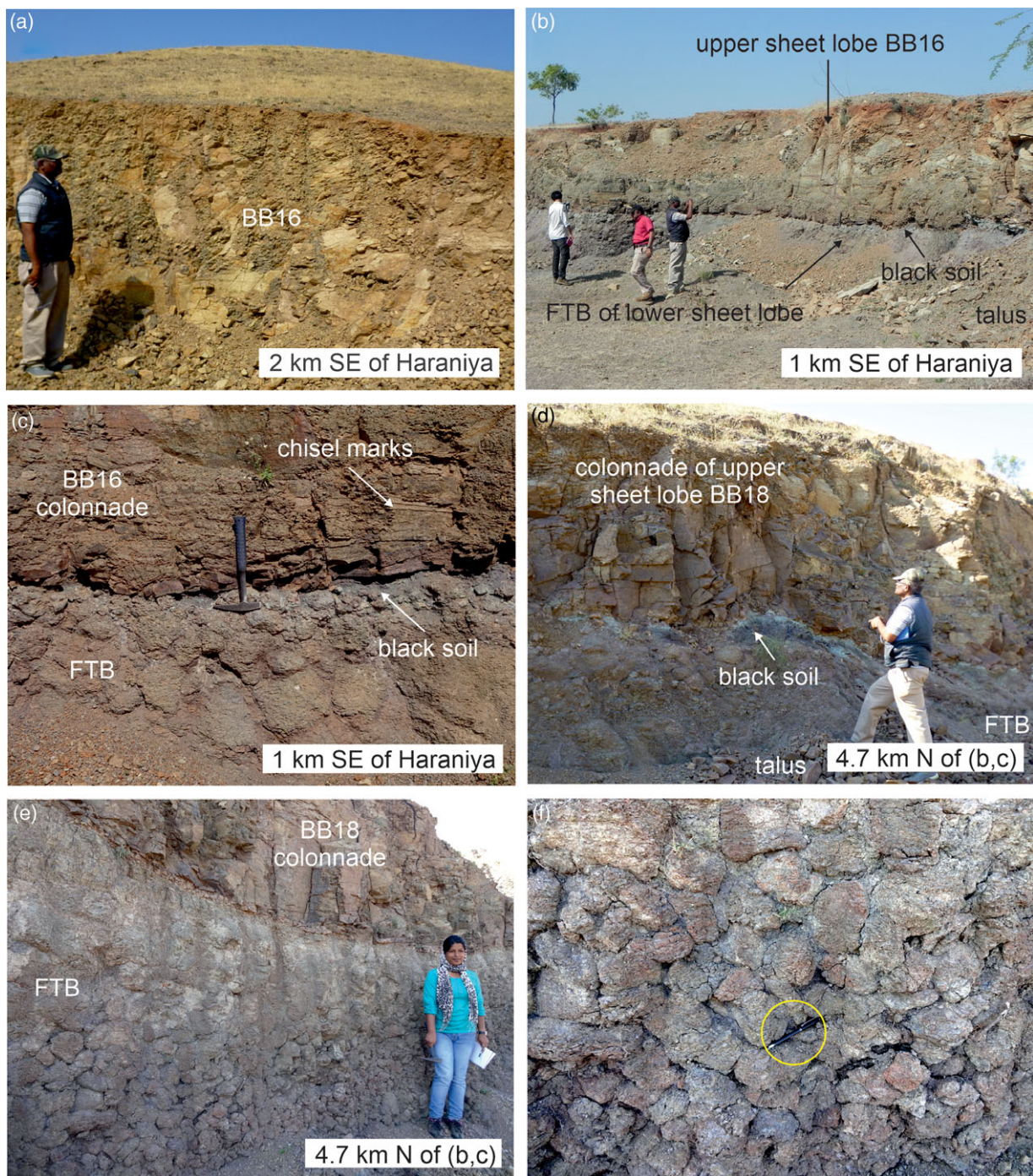
Fig. 7. (Colour online) (a) Sheet lobe BB16 exposed 2 km southeast of Haraniya. Location is 22° 18′ 28.3″ N, 71° 20′ 59.9″ E, 161 m. (b, c) Quarry pit ~1 km southeast of Haraniya, showing BB16 and an underlying sheet lobe. Location is 22° 18′ 39.5″ N, 71° 19′ 28.7″ E, 176 m. FTB is flow-top breccia. Hammer for scale in (c) is 33 cm long. (d, e) The same two sheet lobes 4.7 km N 12° E of the location in (b, c). Location is 22° 21′ 9.9″ N, 71° 20′ 01.8″ E, 199 m. (f) Detail of the flow-top breccia. Vertical section, pen (encircled) for scale is 14 cm long.

shows well-formed, metres-thick basal breccia, a dense core and an overlying entablature tier (Fig. 11a–d).

4. Petrography

Petrographic features of the sheet lobes of our study are generally similar to those of other Saurashtra and Deccan tholeiites (e.g. Sheth *et al.* 2013; Krishnamurthy, 2020). The rock samples are fine grained, with plagioclase and clinopyroxene the dominant minerals, sometimes with olivine (commonly altered) and Fe–Ti oxides. Textures range from aphyric to plagioclase-phyric, as in the lower colonnade of the Bamanbor sheet lobe (Fig. 12a), to highly plagioclase-phyric, as in the Lakhavad sheet lobe BB10. Some of the samples show small vesicles filled by secondary minerals such as quartz and zeolites.

However, large amounts of interstitial glass (20–25 vol. %) are observed along with skeletal, dendritic to axiolitic Fe–Ti oxides in the entablature of the Bamanbor sheet lobe (Fig. 12b–d). Abundant

Fig. 8. (Colour online) (a) Chotila Hill (22° 25′ 10.8″ N, 71° 12′ 35.8″ E, 334 m) with the pre-1884 landslide scar and resultant deposit indicated. (b, c) Dyke segments BB04 and BB08 on the southern lower slopes of Chotila Hill. (d) The landslide deposit with one of the basaltic blocks numbered BB07. Coin for scale is 2.5 cm wide. (e) Short, irregular columns in the entablature of a sheet lobe exposed at the base of Chotila Hill. Vertical section, pen (encircled) for scale is 14 cm long.

olivine (besides clinopyroxene), and highly elongate and skeletal (hollow-cored and swallowtail) crystals of plagioclase, forming feathery and spherulitic growths, are seen in the Chotila dyke (Fig. 13a–f). Tiny spikes of plagioclase have grown on some of the larger plagioclase crystals (Fig. 13e; compare fig. 3.16 of Vernon, 2018). The dyke also shows significant amounts of interstitial glass, with varying concentrations of Fe–Ti oxide microlites within the glass imparting to the glass a colour ranging from brown to black (Fig. 13a–c, e). The dyke shows a few vesicles as well (Fig. 13e).

5. Geochemistry

Small chips of the rock samples were cleaned in an ultrasonic bath and ground to powders of <75 µm grain size using a Retsch PM-100 planetary ball mill and stainless steel grinding balls, in the Department of Earth Sciences, IIT Bombay. Major oxide compositions of the dykes by inductively coupled plasma atomic emission spectrometry (instrument: Jobin Yvon Ultima 2) and loss on ignition (LOI) values were also determined there following the methods described in Sheth *et al.* (2013). The LOI values of the

samples are mostly well over 1 wt %, and reach >4 wt % for BB10. Even higher LOI values have been found for many samples from Moti Gop Hill (5–6 wt % to as much as 9.97 wt % for MG06). The high LOI values for most samples indicate moderate to considerable subaerial weathering and secondary mineralization.

The geochemical data are presented in Tables 1 and 2, along with rock names determined and Mg numbers (Mg#) computed on an anhydrous basis using the SINCLAS program of Verma *et al.* (2002). Of the 34 rock samples analysed, a majority (28) are subalkalic basalts and four are basaltic andesites. These have Mg# values ranging from 68.4 to 40.8 showing that the magmas were moderately evolved. Low-Ti compositions dominate, represented by all 18 samples from Moti Gop Hill (TiO_2 <1.5 wt %; Table 2). The other samples (Table 1) include a few low-Ti, intermediate-Ti (~2 wt % TiO_2) and three high-Ti (~3–3.5 wt % TiO_2) types. All these rocks are well comparable to the bulk of the Deccan tholeiites including those of the Western Ghats sequence (e.g. J. E. Beane, unpub. Ph.D. thesis, Washington State Univ., 1988). However, the Talaja upper sheet lobe SS15 and the sheet lobe SS17 near Longdi are different in being andesitic in bulk composition, with Mg# as low as 38.6.

Fig. 9. (Colour online) Features of a very thick sheet lobe exposed on the National Highway 8B near Bamanbor. (a) Road-cut through a thick entablature (12 m exposed, person for scale). Around this location the entablature is traversed by master joints with a roughly equal spacing of ~6 m, one of which is seen in this photograph. (b) Upper colonnade overlying the entablature tier, with thin but regular, vertical columns. White dashed line shows their gently undulating boundary in part. (c) Vertical joint face in the entablature, exposing many small-scale, irregular joints forming intersecting networks. Photograph courtesy J. M. Sheikh. Compare Figure 4c, d. (d) Detail of the entablature (vertical section, hammer for scale is 33 cm long), showing joints splaying and merging in various orientations. Sample BB03 taken here has the coordinates 22° 25′ 14.1″ N, E 71° 02′ 01.5″ E, 195 m. (e) A rosette of radial joint columns widening away from a narrow central zone or point. Geologist is Tanmay Keluskar. (f) 'The skeleton', a structure formed of short horizontal columns that grew on the two sides of a vertical joint. Note the very irregular jointing of the rest of the entablature in both (e) and (f). (g, h) Well-formed lower colonnade of ~10 m exposed thickness on the Bamanbor–Wankaner road, 18 km south of Wankaner. Sample BB01 taken here has the coordinates 22° 28′ 27.4″ N, 71° 03′ 1.0″ E, 180 m. This colonnade underlies the entablature shown in (a–f). The Bamanbor sheet lobe is thus ≥27 m in thickness. Note person (encircled) for scale in (g), and the many metres-wide individual columns with subhorizontal chisel marks in (h).
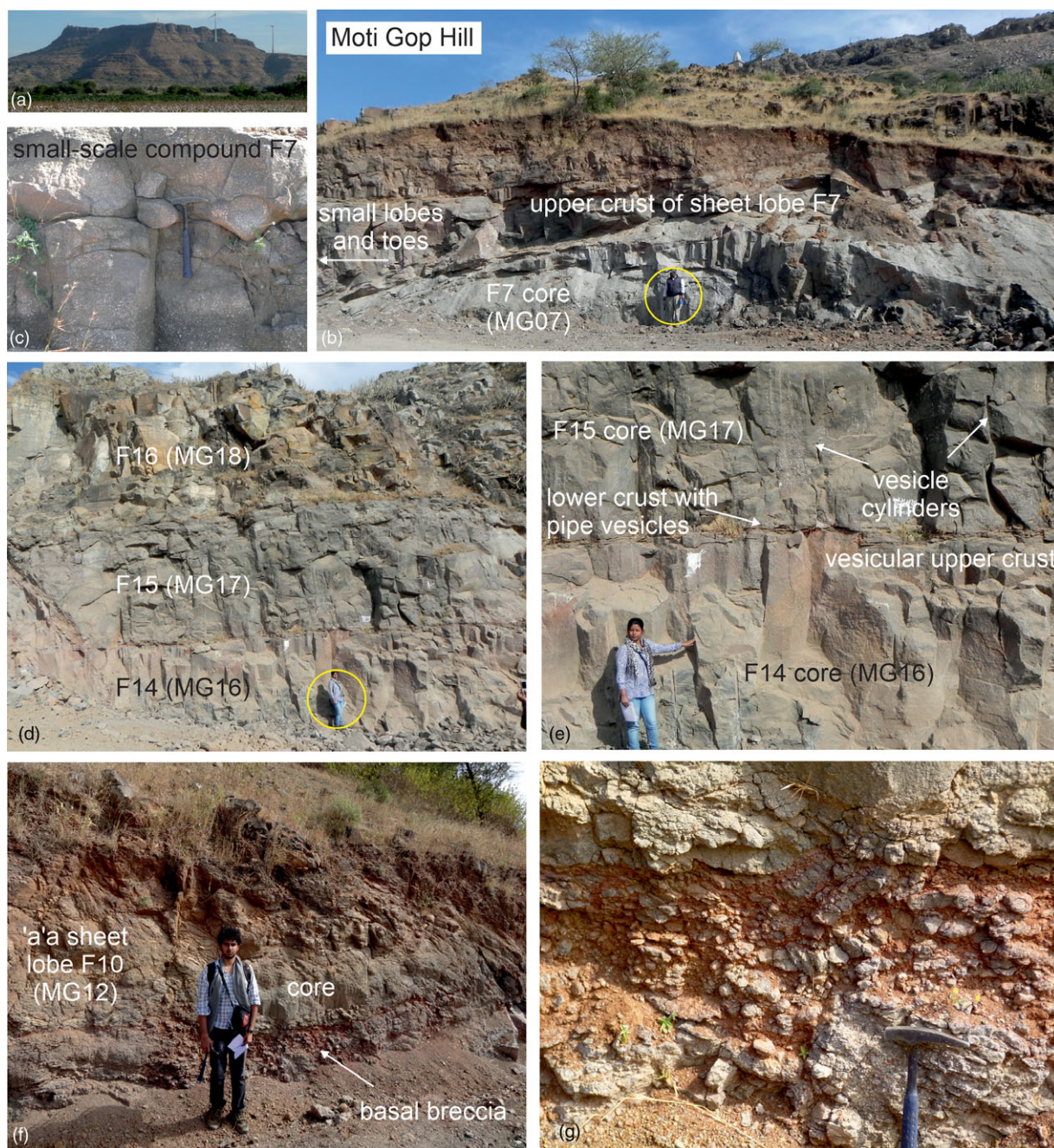
Fig. 10. (Colour online) Features of sheet lobes in the Moti Gop Hill (335 m). (a) Panoramic view of Moti Gop Hill (22° 02′ 47.0″ N, 69° 55′ 35.0″ E, 335 m). Relief is ~220 m. (b) Metres-thick sheet lobe (flow F7) at ~230 m elevation. Person (encircled) for scale. The sheet lobe shows a lateral transition into small-scale compound lobes and toes on the left (north), which are shown in (c). Note highly vesicular-amygdaloidal lobes and toes. Vertical section, hammer for scale is 33 cm long. (d) Stack of uppermost three sheet lobes (F14, F15, F16) at Moti Gop. Note crude subvertical columnar jointing in each; person (encircled) for scale. (e) Closer view of parts of sheet lobes F14 and F15. F14 shows an upper crust with spherical vesicles filled by secondary minerals. F15 shows pipe vesicles at the base and a core with many vesicle cylinders, also filled by secondary minerals. (f) 'A'ā sheet lobe F10 at ~277 m elevation in the Moti Gop Hill. (g) Detail of the basal clinker of the 'a'ā sheet lobe F10, showing partial alteration to red bole.

6. Discussion

6.a. Volcanological interpretations of lava morphotypes

The sheet lobes of this study, while resembling the bulk of the Deccan tholeiites in their petrographic and major-element geochemical characters, constitute various lava morphotypes that reflect the cumulative effects of intrinsic parameters such as composition, temperature, crystallinity and volatile content, and extrinsic parameters such as eruption mechanism, effusion rate, topography and flow velocity (e.g. Peterson & Tilling, 1980; Rowland & Walker, 1990; Kilburn, 2000; Duraiswami *et al.* 2014). Below we discuss our volcanological interpretations of the lava morphotypes.

6.a.1. Sheet lobes versus small-scale compound pāhoehoe flows

As noted, small-scale compound pāhoehoe flows are common and widespread across Saurashtra, whereas sheet lobes are also by no
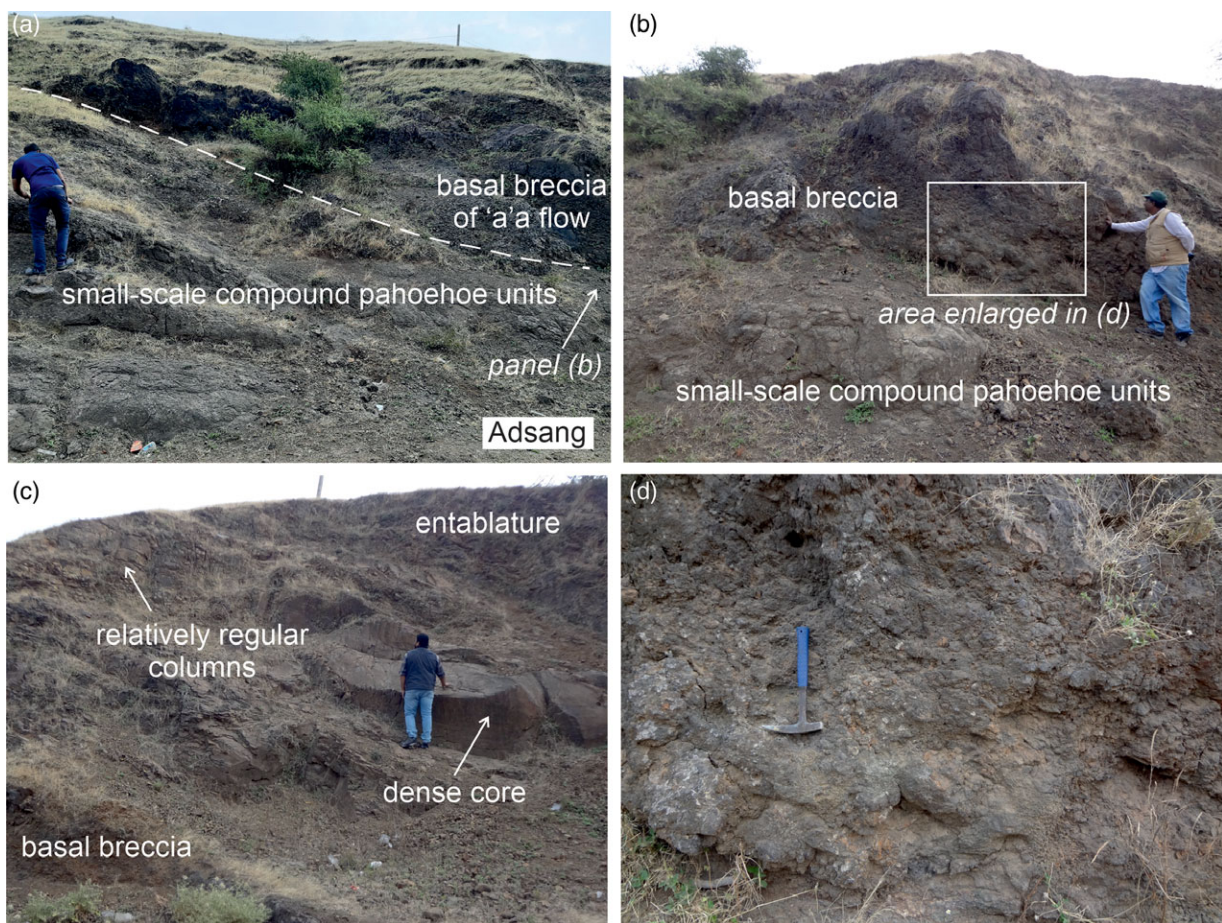
Fig. 11. (Colour online) (a–d) 'A'ā sheet lobe overlying small-scale compound pāhoehoe flow-units at Adsang. Location is 21° 07′ 06.6″ N, 71° 20′ 37.9″ E, 153 m. Hammer for scale is 33 cm long.

means uncommon in the region (Figs 2–11). The absence of characteristically subaqueous pillow lavas or lava–sediment mingling features such as peperites, even in areas with 'intertrappean' sediments (such as Lakhavad–Ninama), shows that the sheet lobes and the small-scale compound flows were entirely subaerial eruptions. However, they may imply very different eruption rates. The sheet lobes are evidently large-volume lava flows, as exemplified by their thicknesses and minimum lateral extents of several kilometres. The correlated sheet lobe BB16–BB18 around Haraniya and north of it (Fig. 7) is at least 5.2 km long. The entablature of the ≥27 m thick Bamanbor sheet lobe is exposed for many kilometres westwards towards Rajkot, whereas towards the east, the same entablature may correlate with that at Chotila (Fig. 8e), 13 km from Bamanbor, as noted from their comparable elevations and horizontality (see also Shekhawat & Sharma, 1996). The Bamanbor sheet lobe also extends at least 6.1 km in an ~N–S direction (the lateral distance between samples BB03 and BB01). The Moti Gop Hill is largely composed of sheet lobes at least a few kilometres long (Fig. 10a). The Talaja, Longdi and Sidsar sheet lobes (Figs 4, 5) were likely originally extensive, though their current outcrop areas are limited owing to significant tectonic dips. In fact, the Talaja sheet lobe SS15 and the Longdi sheet lobe SS17 are probably the same sheet lobe, as suggested by their general appearance including the entablatures with high degrees of alteration, comparable structural dips, petrographic characteristics and, most distinctively, their andesitic bulk compositions, the only ones

in the entire dataset (Table 1). This correlation implies a minimum original length of 18.4 km for the combined SS15–SS17 sheet lobe along a NE–SW direction.

The widespread and voluminous sheet lobes of Saurashtra may indicate large-volume, high-volumetric flux eruptions (see also Reidel *et al.* 2018; Self *et al.* 2021). In contrast the small-scale compound pāhoehoe flows were formed from low-volumetric flux eruptions similar to modern Hawaiian eruptions, though the total volumes of individual eruptions were orders of magnitude larger than for modern Hawaiian lavas (e.g. Walker, 1971; Sheth *et al.* 2017b; Sheth, 2018; see also Jay *et al.* 2018). It is also probable that some of the sheet lobes transitioned laterally into small-scale compound pāhoehoe flows, as seen in the lateral transition of Moti Gop sheet lobe F7 into small units and toes over a distance of tens of metres (Fig. 10b, c). Such a transition is expected in the distal parts or terminus of a sheet lobe, where the lobe (whether 'cooling-limited' or 'volume-limited'; Pinkerton & Wilson, 1994) has extensively solidified and stopped moving (see also Keszthelyi & Self, 1998; Vye-Brown *et al.* 2013).

6.a.2. Pāhoehoe sheet lobes

Pāhoehoe and 'a'ā (Macdonald, 1953; Peterson & Tilling, 1980; Rowland & Walker, 1990; Harris *et al.* 2017) are two fundamental and widespread morphological types of basaltic lava. Most lava flows in a flood basalt province such as the Deccan Traps are pāhoehoe, a lava morphotype which is highly fluid and favoured
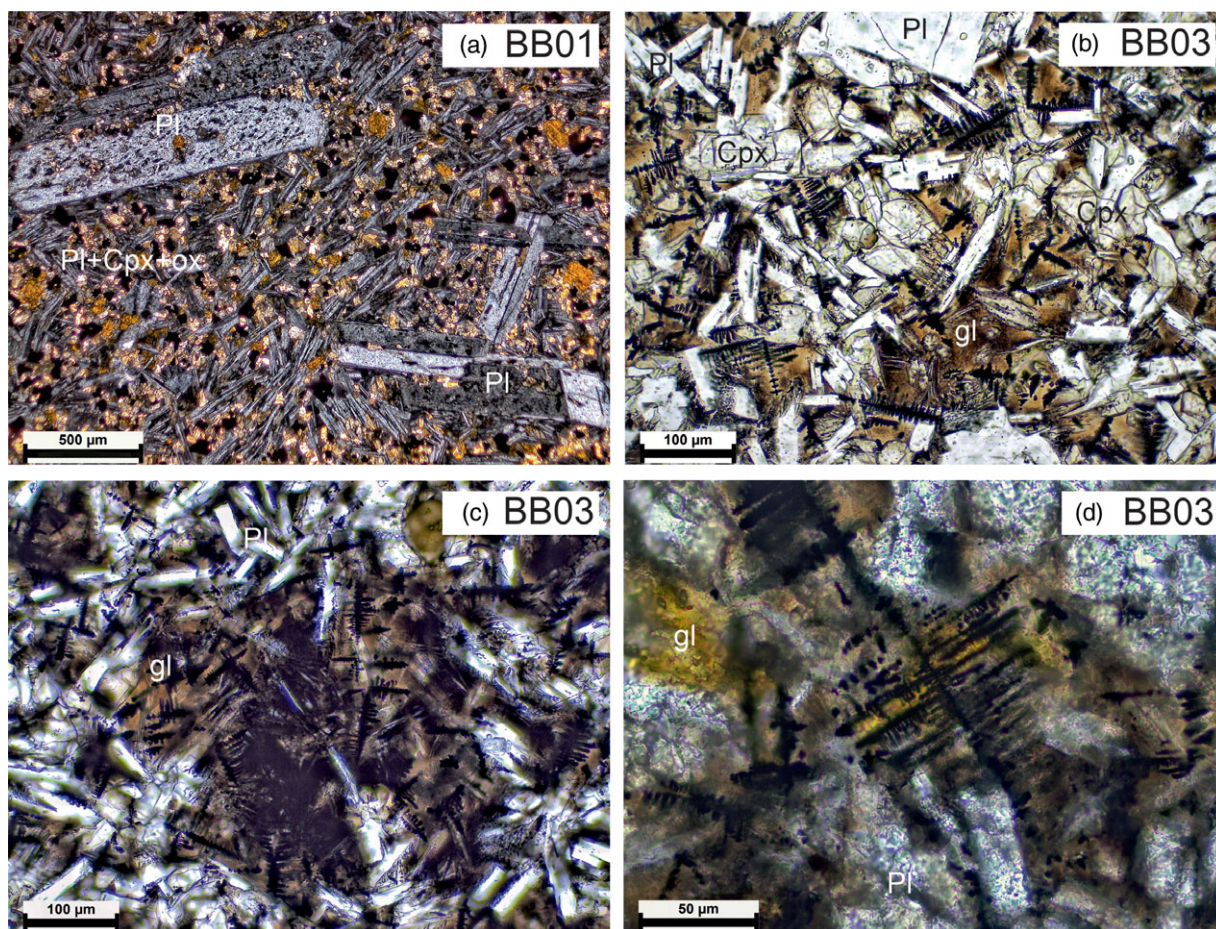
Fig. 12. (Colour online) Thin-section photomicrographs showing representative views of the colonnade and entablature of the Bamanbor sheet lobe under the petrological microscope. Plagioclase (Pl) grains (both phenocrysts and in the groundmass) are lath-shaped, and the clinopyroxene (Cpx) grains are equant. (a) Sample BB01 from the colonnade, cross-polarized light. Note the well-formed crystals, equant shapes of the abundant small Fe–Ti oxide grains (black) and absence of glass. (b–d) Sample BB03 from the entablature, plane-polarized light. Note the acicular, dendritic and skeletal shapes of the abundant Fe–Ti oxide grains (black). Note also the large amounts of interstitial glass (b, c), a cluster of many oxide grains (c) and an axiolite with spikes growing on either side of a central axis of a Fe–Ti oxide grain (d).

by low strain rates (as prevail with low ground slopes and flow velocities). Pāhoehoe flows grow mainly endogenously, i.e. lava is transported under a thick solidified crust in lava tubes, thus efficiently retaining heat and travelling long distances from the eruptive vent if the erupted volume is large. Each lobe develops an upper crust solidifying downwards which captures rising buoyant gas bubbles and is therefore highly vesicular, whereas the underlying core is vesicle-poor. Lateral enlargement and swelling of the lobe occurs by periodic injection of new lava under the crust, termed inflation (Macdonald, 1953; Self *et al.* 1997), with the final lobe thickness many times the initial emplacement thickness.

The upper sheet lobe at Talaja (Fig. 4a–d), the sheet lobe near Longdi (Fig. 5a), the Lakhavad sheet lobe (Fig. 6a, b) and the thick Bamanbor sheet lobe (Fig. 9) are pāhoehoe lava flows, at least at face value (their upper parts including any original flow-top breccia have been eroded or quarried). In the Moti Gop Hill, flow F7 is a thick pāhoehoe sheet lobe with a columnar-jointed upper crust and a dense core (Fig. 10b) whose lateral transition into small lobes and toes was described above. Flow F15 near the top of the section is similarly a pāhoehoe sheet lobe 5 m thick. It contains pipe vesicles in its thin basal crust, an abundance of vesicle cylinders in its core, and a vesicular upper crust (Fig. 10d, e). The spherical vesicles in the upper crust indicate trapping of upward-rising gas bubbles by the downward-solidifying upper crust (Aubele *et al.* 1988). Pipe vesicles have been variously ascribed to rising buoyant gas bubbles (Walker, 1987), gas bubbles trapped within inward-moving solidification fronts (Philpotts & Lewis, 1987) and droplets of dense, immiscible iron- and sulphide melts sinking in the highly crystalline, mushy basal lava (Sheth, 2020). The vesicle cylinders are vertically elongated cylindrical zones of bubble-rich, compositionally evolved lava left after advanced crystallization; this late-stage, residual lava rises buoyantly and diapirically from the lower part of the sheet lobe into its still-molten (but stationary) core (Goff, 1996; Barreto *et al.* 2017). The sheer abundance of the vesicle cylinders in sheet lobe F15 suggests a volatile-rich basaltic lava.

6.a.3. Rubbly pāhoehoe sheet lobes

Rapid inflation of a pāhoehoe lava lobe with fracturing of the lava crust leaves the crust broken into slabs and produces the lava morphotype slabby pāhoehoe (Duraiswami *et al.* 2003). Brecciation of the slabs produces flow-top breccia and the lava morphotype rubbly pāhoehoe (Keszthelyi & Thordarson, 2000; Duraiswami *et al.* 2008). The lava morphotypes slabby pāhoehoe (not found in our study area) and rubbly pāhoehoe (common in our study area) are thus transitional between
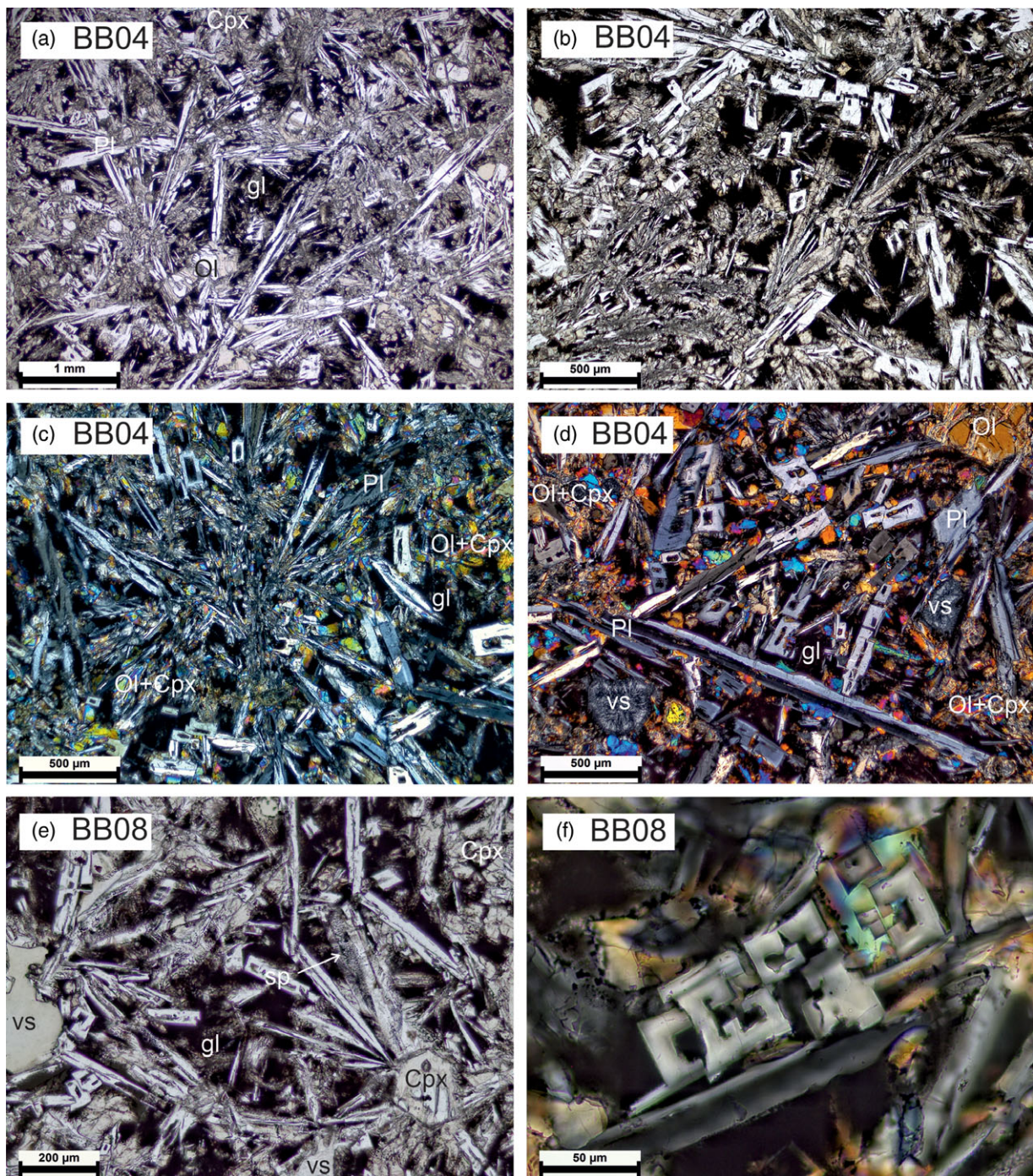
Fig. 13. (Colour online) Thin-section photomicrographs showing representative views of the Chotila Hill dyke segments BB04 and BB08 under the petrological microscope. Views (a, b, e) are in plane-polarized light, and the others in cross-polarized light in which olivine (Ol) and clinopyroxene (Cpx) display brilliant second-order colours and plagioclase (Pl) shows shades of grey. Dark to black areas are interstitial glass (gl) with varying abundance of microlites of Fe–Ti oxides. Vesicles filled by secondary minerals are indicated by 'vs'. Note the highly elongate, acicular and skeletal (hollow-cored to swallowtail) plagioclase grains which form feathery to spherulitic arrangements (a–e), and the innumerable tiny spikes (sp) overgrowing several plagioclase laths in (e). Panel (f) shows a cluster of skeletal plagioclase grains cut perpendicular to their *c* axes, several of which are also seen in the other panels, especially (d).

pāhoehoe and ʻaʻā. Unlike pāhoehoe flows, with unbroken upper crusts, these have extensively fractured and brecciated upper crusts, but all three types have preserved bases implying that they do not thermally or mechanically erode their substrates. Rubbly pāhoehoe has been considered the most common lava morphotype in the Deccan Traps (Duraiswami *et al.* 2008), though it has not yet been described from the Saurashtra region.

The rubbly pāhoehoe flows we have described here include the lower sheet lobes of Talaja (Fig. 4b, e, f), Sidsar (Fig. 5f) and Haraniya (Fig. 7), and most of the Moti Gop Hill, including sheet lobes F1, F4, F5, F6, F8, F12, F14 and possibly F2 and F16 (Fig. 10; online Supplementary Material Table S2). We consider that all these rubbly pāhoehoe lavas were initially emplaced as pāhoehoe (Fig. 14a), but their viscoelastic crusts experienced shearing and

Table 1. Major oxide geochemical data (in wt.%) and CIPW norms (in wt.%) of sheet lobes and associated dykes of Saurashtra, Deccan Traps

Location	Tal	Lon	Sid	Bam	Bam	Cho	Cho	Cho	Pip	Lak	Har	Ada	std	std	std	std
Comp.	A	A	BA	B, sa	BA	B, sa	B, sa	B, sa	B, sa	B, sa	B, sa	B, sa	Ref.	Meas.	Ref.	Meas.
Sample	**SS15**	**SS17**	**Sid01**	**BB01**	**BB03**	**BB04**	**BB07**	**BB08**	**BB09**	**BB10**	**BB16**	**BB18**	**BHVO2**	**BHVO2**	**W2a**	**W2a**
SiO_2	55.54	60.49	54.13	47.68	52.10	48.91	48.74	50.05	48.49	44.36	52.65	52.97	49.90	48.79	52.68	54.54
TiO_2	1.98	1.60	1.69	3.44	1.63	1.09	1.26	1.04	3.05	2.84	2.19	2.10	2.73	2.75	1.06	1.11
Al_2O_3	9.36	9.32	14.04	13.21	13.86	13.26	14.69	12.74	14.63	16.45	13.37	13.15	13.50	12.94	15.45	15.67
Fe_2O_{3T}	12.58	11.82	13.71	16.31	14.81	12.07	12.23	12.03	13.87	13.18	11.92	11.79	12.30	12.23	10.83	10.85
MnO	0.18	0.17	0.20	0.22	0.21	0.18	0.24	0.18	0.29	0.21	0.17	0.17	0.17	0.17	0.17	0.17
MgO	3.73	2.86	5.17	5.38	4.82	11.17	6.54	10.70	5.13	3.89	6.45	6.60	7.23	7.14	6.37	6.40
CaO	7.12	5.41	9.02	9.87	8.58	10.11	10.75	9.59	9.06	9.04	8.56	8.40	11.40	11.18	10.86	10.88
Na_2O	2.76	2.74	2.43	2.44	2.36	1.54	2.33	1.63	2.45	2.61	2.15	2.21	2.22	2.04	2.20	2.18
K_2O	2.04	3.03	0.73	0.87	0.97	0.12	0.63	0.38	1.02	0.92	1.53	2.22	0.52	0.39	0.63	0.72
P_2O_5	0.23	0.24	0.16	0.42	0.20	0.12	0.17	0.09	0.44	0.55	0.27	0.28	0.27	0.26	0.14	0.10
LOI	1.45	1.80	1.05	1.87	1.39	2.02	1.38	2.39	2.70	4.36	2.40	1.96	–	–	–	–
Total	97.00	99.47	102.33	101.71	100.93	100.59	98.96	100.82	101.13	98.41	101.66	101.85	100.24	97.89	100.38	102.62
Mg#	43.6	38.6	48.7	43.5	45.0	68.4	55.6	67.5	46.4	40.8	57.7	58.5				
Q	13.27	18.32	8.66	0.23	6.87	–	–	1.01	2.06	–	6.57	4.43				
Or	12.77	18.47	4.30	5.22	5.83	0.73	3.85	2.31	6.20	5.85	9.20	13.26				
Ab	24.66	23.93	20.52	20.97	20.30	13.36	20.42	14.16	21.32	23.76	18.51	18.90				
An	7.55	4.36	25.20	22.88	24.76	29.64	28.76	27.03	26.64	32.77	22.69	19.61				
Di	23.43	18.23	15.24	20.02	14.30	16.98	20.85	17.20	13.77	9.70	15.25	16.82				
Hy	9.17	8.73	18.28	19.40	19.68	33.06	18.73	33.34	19.86	13.55	19.19	18.64				
Ol	–	–	–	–	–	1.09	1.70	–	–	4.05	–	–				
Mt	4.62	4.24	4.22	3.66	4.64	2.74	2.80	2.73	3.15	3.14	3.74	3.67				
Il	3.98	3.15	3.20	6.64	3.15	2.12	2.48	2.03	5.96	5.80	4.23	4.03				
Ap	0.57	0.57	0.37	0.99	0.47	0.29	0.41	0.21	1.05	1.37	0.64	0.66				

Notes: The samples represent the following rock units: SS15, entablature of upper sheet lobe near Talaja; SS17, entablature of sheet lobe near Longdi; Sid01, colonnade of upper sheet lobe at Sidsar; BB01 and BB03, lower colonnade and entablature of sheet lobe around Bamanbor; BB09, base of flow overlying Mesozoic sandstone near Piparali (at location N 22° 24' 10.5", E 71° 17' 12.8, 192 m); BB10, top of colonnade of highly plagioclase-phyric sheet lobe at Lakhavad; BB16, entablature of sheet lobe near Haraniya; BB18, colonnade of sheet lobe near Adala; BB16 and BB18 represent the same sheet lobe underlain by black soil and flow-top breccia of a lower flow. BB07, basalt block in debris flow deposit at Chotila Hill, southern side; BB04 and BB08, two segments of an en echelon dyke exposed on southern lower slopes of Chotila Hill. All sheet lobes are pāhoehoe. Compositions "B, sa", "BA" and "A" mean subalkalic basalt, basaltic andesite, and andesite, respectively. Mg# = 100 Mg^{2+}/(Mg^{2+} + Fe^{2+}), atomic, where Fe^{2+} and Fe^{3+} are computed following Middlemost (1989). Reference and measured values for the USGS standards BHVO2 and W2a (Wilson, 2000) provide an idea about analytical accuracy.

Table 2. Major oxide geochemical data (in wt.%) and CIPW norms (in wt.%) of the lava flows and a dyke of Moti Gop Hill, Saurashtra, Deccan Traps

Flow	F1	F2	F3	F4	F5	F6	F7	F8	F9	Dyke	F9	F10	F11	F12	F13	F14	F15	F16
El. (m)	119	164	199	201	209	215	230	238	244	255	267	277	280	290	300	309	323	324
Comp.	B, sa	B, sa	B, sa	B, sa	B, sa	B, sa	B, sa	B, sa	B, sa	B, sa	B, sa	B, sa	B, sa	B, sa	B, sa	BA	B, sa	BA
Sample	**MG01**	**MG02**	**MG03**	**MG04**	**MG05**	**MG06**	**MG07**	**MG08**	**MG09**	**MG10**	**MG11**	**MG12**	**MG13**	**MG14**	**MG15**	**MG16**	**MG17**	**MG18**
SiO_2	45.99	48.63	48.08	48.02	47.58	43.97	45.39	46.96	46.98	49.51	46.54	47.71	49.28	48.99	48.35	48.30	47.63	48.01
TiO_2	1.10	1.48	0.83	0.66	0.76	1.21	1.10	0.92	1.00	0.89	1.04	1.12	1.19	1.12	0.80	0.83	0.76	0.89
Al_2O_3	15.55	14.35	13.18	12.84	13.92	14.09	13.61	14.27	14.27	14.17	14.57	15.36	15.54	14.76	14.62	13.70	14.60	13.92
Fe_2O_{3T}	12.06	13.40	12.74	11.27	12.75	11.98	12.23	11.92	12.28	12.22	12.85	12.71	12.45	13.03	12.22	12.72	12.11	13.75
MnO	0.18	0.23	0.21	0.16	0.20	0.18	0.21	0.18	0.19	0.20	0.20	0.18	0.20	0.20	0.20	0.20	0.19	0.22
MgO	9.43	5.55	7.19	6.80	6.58	4.95	5.69	6.67	6.88	6.10	5.71	5.81	5.97	5.98	7.51	7.08	6.32	7.08
CaO	10.36	11.65	12.15	12.11	12.75	11.27	12.39	12.36	12.48	11.78	12.06	12.58	11.66	12.05	13.63	13.34	12.39	12.65
Na_2O	2.30	2.49	2.56	1.58	1.72	1.15	2.07	1.85	1.99	2.14	1.99	2.16	2.20	1.89	1.64	1.64	2.02	2.00
K_2O	0.20	0.37	0.60	0.12	0.22	0.17	0.25	0.33	0.37	0.17	0.16	0.30	0.30	0.99	0.04	0.20	0.04	0.21
P_2O_5	0.09	0.30	0.20	0.12	0.12	0.15	0.26	0.20	0.17	0.11	0.17	0.16	0.08	0.14	0.12	0.08	0.06	0.07
LOI	1.89	0.86	3.00	6.16	1.48	9.97	5.08	2.69	1.82	1.53	2.91	2.05	1.76	2.87	2.97	3.56	5.84	1.95
Total	99.15	99.31	100.74	99.84	98.08	99.09	98.28	98.35	98.43	98.82	98.20	100.14	100.63	102.02	102.10	101.65	101.96	100.75
Mg#	64.6	49.2	56.9	58.5	54.7	49.1	52.1	56.7	56.7	53.9	51.0	51.7	52.8	51.8	59.0	56.5	55.0	54.6
Q	–	–	–	3.55	0.04	4.67	–	–	–	2.17	–	–	0.74	–	–	–	–	–
Or	1.23	2.25	3.67	0.76	1.36	1.14	1.60	2.06	2.29	1.05	1.01	1.83	1.81	5.97	0.24	1.22	0.25	1.27
Ab	20.22	21.65	22.41	14.42	15.24	11.04	19.01	16.54	17.62	18.81	17.87	18.84	19.03	16.31	14.15	14.30	17.97	17.33
An	32.75	27.63	23.49	29.76	31.00	37.21	29.41	31.33	30.25	29.67	32.22	32.30	32.35	29.44	33.04	30.34	32.24	29.08
Di	16.31	24.69	30.88	28.08	28.40	20.87	29.32	26.39	27.45	25.03	24.97	25.63	21.70	25.33	28.80	30.75	26.40	28.67
Hy	6.83	16.36	1.97	19.09	19.21	19.06	10.86	16.36	10.89	18.44	17.69	12.00	19.06	15.96	17.42	18.63	18.31	12.78
Ol	17.50	0.77	12.56	–	–	–	3.94	2.20	6.27	–	0.71	3.94	–	1.55	1.77	0.05	0.36	5.86
Mt	2.77	3.04	2.91	2.69	2.95	3.01	2.93	2.79	2.84	2.81	3.02	2.90	2.81	2.94	2.75	2.90	2.82	3.11
Il	2.17	2.89	1.63	1.35	1.51	2.61	2.27	1.85	1.99	1.76	2.10	2.19	2.31	2.17	1.55	1.63	1.52	1.73
Ap	0.22	0.71	0.48	0.30	0.29	0.39	0.65	0.49	0.41	0.26	0.42	0.38	0.19	0.33	0.28	0.19	0.15	0.17

Notes: All flows are sheet lobes, except F3 (small-scale compound pāhoehoe) and F9 (large-scale compound and columnar). Sheet lobe F7 laterally transitions into small-scale flow units. All sheet lobes are pāhoehoe, except F10 which is 'a'ā (see Table 1). El. (m) indicates elevation of the specific MGxx samples in meters above mean sea level. Samples MG09 and MG11 are from the same flow (F9), and sample MG10 is from a dyke found intruding F9. Compositions "B, sa" and "BA" mean subalkalic basalt and basaltic andesite, respectively. Mg# = 100 $Mg^{2+}/(Mg^{2+} + Fe^{2+})$, atomic, where Fe^{2+} and Fe^{3+} are computed following Middlemost (1989). Reference and measured values for USGS standards are as provided in Table 1.
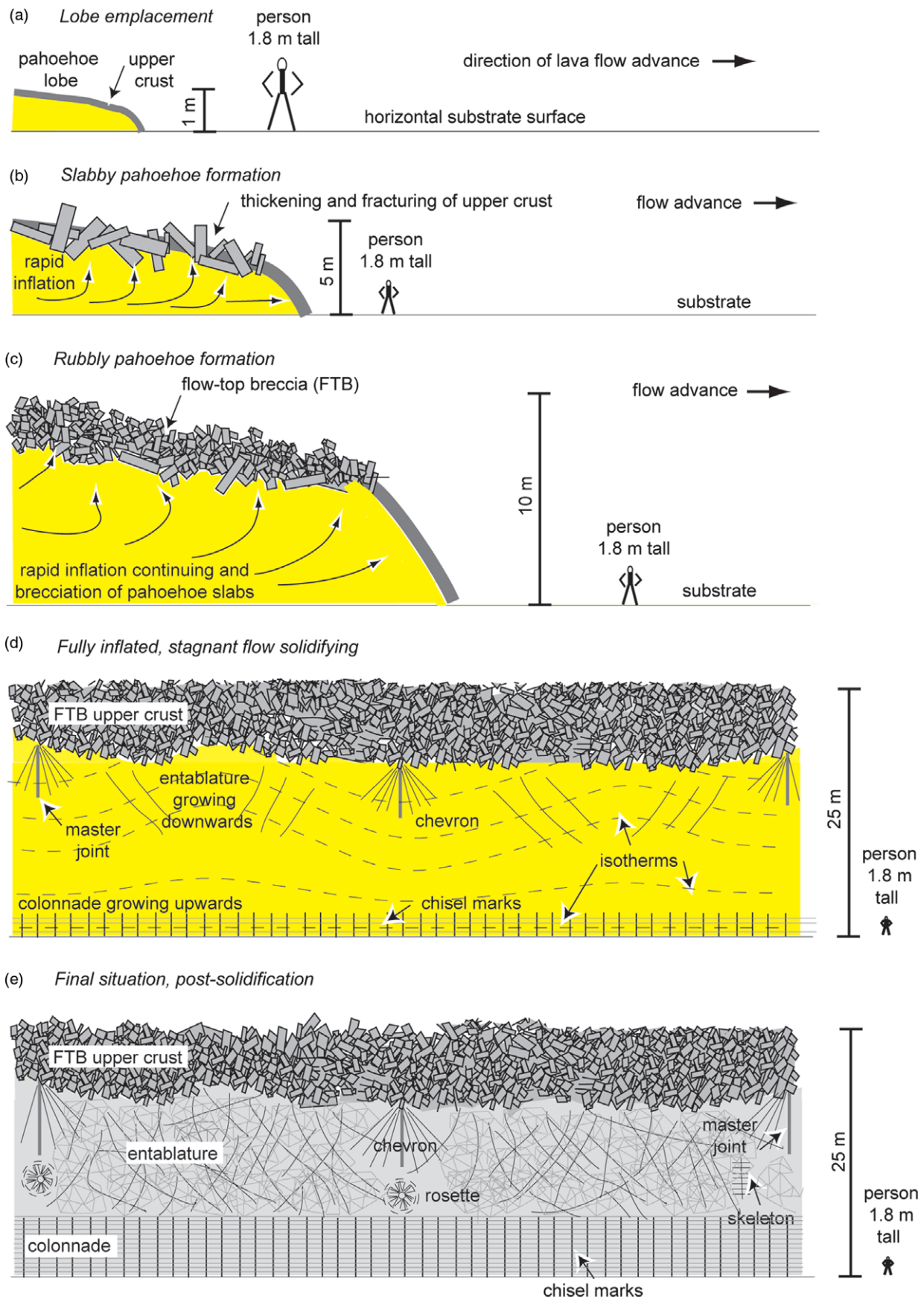
Fig. 14. (Colour online) (a–e) A series of cartoons schematically illustrating the concepts of the formation of lava morphotypes slabby pāhoehoe and rubbly pāhoehoe, and of entablature and colonnade tiers in sheet lobes (here of rubbly pāhoehoe). (a) A small pāhoehoe lobe being emplaced develops an upper crust. (b) The lobe rapidly inflates and its upper crust undergoes stretching and fracturing, producing slabby pāhoehoe. (c) Further rapid inflation leads to brecciation of the slabs, producing rubbly pāhoehoe with flow-top breccia (FTB). New FTB continues forming as the lobe continues to rapidly inflate. (d) The fully inflated and largely molten (except for the thick FTB) sheet lobe, with the shapes of the isotherms (dashed lines) within the lobe controlling the geometry of columnar joint sets. The whole molten interior is shown in one colour (bright yellow) for simplicity. The isotherms in the upper part are undulating due to meteoric water ingress into the sheet lobe through the FTB and along master joints, but horizontal near the sheet lobe's base. Chevrons and rosettes of columns form in orientations perpendicular to the local isotherm configurations. (e) The completely solidified sheet lobe with a thick FTB, a thick entablature with highly irregular columnar joint and fracture sets, and a thinner colonnade below. A typical thickness of the lobe or flow at every stage is also shown, though there is a range of thicknesses at which the behaviour displayed can be reached. A human figure (1.8 m tall) is added to the lower right corners of panels (a) through (e) so that the reader can easily visualize the scales of the sheet lobes. Small features such as chisel marks in the colonnade and small-scale fractures in the entablature are necessarily shown at magnified and disproportionate size so as to be visible.

tearing when the flux of the lava greatly increased, causing rapid flow inflation (Fig. 14b). Such a situation may have resulted from greatly increased lava flux owing to a widened eruptive fissure, or from lava temporarily ponded or dammed in a part of the lava flow being suddenly released in the downflow direction (e.g. Peterson & Tilling, 1980). The consequent crustal stretching and extensional fracturing formed slabby pāhoehoe in which the crustal slabs rotated, collided and fractured further as the flow advanced (Fig. 14b), followed by intense brecciation of the pāhoehoe slabs (Fig. 14c) (Duraiswami *et al.* 2003; Kilburn, 2004; Marshall *et al.* 2016). This produced flow-top breccia and a continuously inflating lobe of rubbly pāhoehoe (Fig. 14c).

The rubbly pāhoehoe sheet lobes found in our study area also throw light on the problem of the origin of bole beds. Duraiswami *et al.* (2020) concluded that bole beds (most commonly red or brown and of closely similar outcrop appearance) may have very diverse origins: they may represent altered glassy bases of basaltic flows, palaeosols formed from weathered flow tops and flow-top breccias, volcanic ash beds, interflow sediments, or altered flow-bottom breccias in rubbly pāhoehoe and ʻaʻā lava flows. They point out that red boles abound in regions of the Deccan Traps dominated by sheet lobes, especially the rubbly pāhoehoe sheet lobes (with flow-top breccias) and ʻaʻā sheet lobes (with flow-top and flow-bottom breccias), and are generally absent within small-scale compound pāhoehoe flows which characteristically lack such breccias. In our study area, observations of the Talaja brown bole bed overlying a rubbly pāhoehoe sheet lobe at Talaja (Fig. 4b, e, f), and the partial conversion to red bole of the basal breccia of the Moti Gop ʻaʻā sheet lobe F10 (Fig. 10f), appear consistent with the mechanism of bole formation from flow-top and flow-bottom breccias proposed by Duraiswami *et al.* (2020).

6.a.4. ʻAʻā sheet lobes

Morphological transitions within individual lava flows, from pāhoehoe to slabby pāhoehoe and further to rubbly pāhoehoe and even ʻaʻā, are well documented in the Deccan Traps (Duraiswami *et al.* 2003, 2014; Sen, 2017). Such transitions can be produced due to increases in eruption rate, flow velocity and strain rate, which all have the effect of destroying (brecciating) any new upper crust immediately as it forms (e.g. Macdonald, 1953; Rowland &Walker, 1990; Kilburn, 2004; Duraiswami *et al.* 2014; Harris *et al.* 2017). This implies that ʻaʻā flows move in open channels with significant heat loss and resultant high lava viscosity. An eruption may produce an ʻaʻā flow directly under conditions of high lava viscosity, high eruption rate and steep ground slopes (e.g. Rowland & Walker, 1990; Brown *et al.* 2011).

As mentioned by Walker (1971), ʻaʻā flows can be compound much like pāhoehoe flows, or they can be simple flows. ʻAʻā flows are uncommon in the Deccan Traps, an important reason being the low ground slopes (<<1°) on which the flows were emplaced, which prevented channelization and ʻaʻā formation. However, some ʻaʻā sheet lobes are encountered in the Western Ghats (Brown *et al.* 2011; Duraiswami *et al.* 2014; fig. 3.84 of Sheth, 2018). In the present study area, sheet lobe F10 in the Moti Gop Hill (Fig. 10f) and the sheet lobe at Adsang (Fig. 11a–d) are ʻaʻā flows. These suggest some combination of high lava viscosities and eruption rates and steep topographic slopes, and ʻaʻā flows in the Deccan Traps may be more common than generally thought.

6.b. Jointing patterns and textures as guides to cooling histories and palaeoclimates

Columnar-jointed sheet lobes of tabular geometry are common in various CFB provinces, including the Deccan Traps (e.g. Long & Wood, 1986; Puffer & Student, 1992; Williamson & Bell, 1994; Lyle, 2000; Jerram, 2002; Sengupta & Ray, 2006; Passey & Bell, 2007; Duraiswami *et al.* 2008; Reidel *et al.* 2013; Schöbel *et al.* 2014; Sheth, 2018; Kale *et al.* 2022). The sheet lobes studied here, besides showing several morphotypes, also show varied jointing patterns which provide clues to their cooling and solidification histories under particular palaeoclimatic conditions. Below we discuss our volcanological interpretations of the various jointing patterns.

6.b.1. Entablature and colonnade tiers

In the simplest situation of conductive cooling, a sheet lobe solidifies from the top inwards and from the bottom upwards, and develops a single tier with columnar jointing, namely a colonnade (the Type I flows of Long & Wood, 1986). Another simple and common situation is that of a two-tiered sheet lobe with an entablature and a colonnade, in which the entablature grows rapidly downward by convective cooling, due to the entry of meteoric water (such as rain) into the upper part of the solidifying sheet lobe. The water enters the lava flow along master joints. Heat is rapidly removed by the resulting steam convection in the entablature, an inference supported by observations of the irregular jointing and quenching suggested by large amounts of glass in the solidified lava (Long & Wood, 1986; Budkewitsch & Robin, 1994; Grossenbacher & McDuffie, 1995; Lyle, 2000; see Fig. 12b–d). The underlying colonnade, which does not interact with the meteoric water, grows much more slowly upward by conductive cooling, and is as a result much thinner than the entablature (Tomkeieff, 1940; Long & Wood, 1986; Lyle, 2000). The last part of the sheet lobe to solidify is the boundary between the entablature and the colonnade. These are the Type III flows of Long & Wood (1986).

More complex cases involve multitiered sheet lobes, with a central entablature between two colonnades (reflecting early conductive cooling from the top and bottom of a lobe during a dry season, followed by meteoric water ingress during the wet season), or a number of entablature and colonnade tiers formed over several years with alternating wet and dry seasons (the Type II flows of Long & Wood, 1986; Lyle, 2000).

The subaerially emplaced tholeiitic sheet lobes of Saurashtra described in this study, with well-formed entablatures and colonnades, represent varied types of columnar jointing, and also contain a number of additional internal structures that are a guide to the emplacement and palaeoclimatic conditions. The thick colonnade of the sheet lobe at Lakhavad (Fig. 6a) is directly overlain by intertrappean limestone. Lacking an entablature altogether, this sheet lobe corresponds to the Type I flows of Long & Wood (1986) that represent the simplest case of purely conductive cooling. This sheet lobe formed by simultaneous upward and downward growth of the colonnade without any involvement of meteoric water (such as rain, or flooding by a displaced stream; Saemundsson, 1970). The two sets of columns would have merged a little below the median plane of the lobe, given that cooling from the top down should have been faster compared to cooling from the bottom up. Joint columns grow by incremental crack propagation perpendicular to the isotherms (contours of equal temperature in a cooling lava), because this is the direction of maximum thermal gradient in the lava (Grossenbacher & McDuffie, 1995).

The horizontal disposition of the isotherms and the purely conductive, slow cooling are indicated by the well-formed, metres-wide, vertical columns with chisel marks.

The top of the Sidsar upper sheet lobe (Fig. 5d, e) has been quarried, and it is not known if its exquisitely formed colonnade was originally overlain by an entablature. This colonnade also reflects conductive cooling under dry environmental conditions, or at least those depths in the solidifying flow which could not be reached by any meteoric water entering from above. Moti Gop sheet lobes such as F14 and F15 also lack entablatures (Fig. 10d, e), and their colonnades are poorly developed, possibly because of their relative thinness (5 m) and thus exposure to the atmosphere. Sheet lobe F14 is also a rubbly pāhoehoe lobe, whose flow-top breccia may have permitted easy meteoric water ingress leading to rapid cooling of the lobe.

The Talaja upper sheet lobe SS15 and its probable lateral equivalent SS17 near Longdi show thick entablature tiers overlying a colonnade (Figs 4a–e, 5a), and correspond to the Type III flows of Long & Wood (1986). We interpret them to have formed by simultaneous upward growth of the colonnade by conductive cooling and much faster downward growth of the entablature by convective cooling due to meteoric water ingress. This ingress occurred along early formed fractures and master joints, and strongly affected the temperature distribution within what was to become the entablature tier (Fig. 14d). The isotherms in the entablature tier became highly distorted, which led to the growth of the columnar joints, besides a range of fractures, in various directions without any regular pattern. The same is true of the entablature exposed at the base of Chotila Hill (Fig. 8e).

The ≥27 m thick Bamanbor sheet lobe (Fig. 9a–h), on the other hand, is a multitiered sheet lobe, with upper and lower colonnades separated by an entablature, and corresponds to the Type II flows of Long & Wood (1986). We interpret this lobe to have begun solidifying by conductive cooling during a dry season (forming the lower and the upper colonnades), followed by meteoric water ingress through the upper colonnade into the lobe interior during the wet season (forming the thick entablature). As noted, the upper colonnade (Fig. 9b, c) has much thinner columns than the lower colonnade (Fig. 9g, h), consistent with the much faster (though still conductive) heat loss from the former, open to the atmosphere unlike the latter.

6.b.2. Chevron, rosette and 'skeleton' jointing in the entablatures

As noted the regular, relatively thick vertical columns in the colonnade of a flat-lying sheet lobe reflect horizontal isotherms. In contrast, the random and irregular orientations and narrow widths of columns, in the entablature of a sheet lobe, indicate highly distorted isotherms due to ingress of meteoric water and rapid cooling (Fig. 14d). Any particular isotherm (say 1000 °C) would be depressed under areas of water ingress in the flow, and elevated in the areas in between. The columns must grow everywhere perpendicular to the local shape of the isotherms. The resulting *chevron jointing* (columns diverging outward and downward from a point) therefore indicates isotherms which are broadly undulating and cuspate due to ingress of meteoric water into the solidifying flow (Fig. 14d) (see fig. 10 in Lyle, 2000; Philpotts & Dickson, 2002). Well-developed chevron jointing is observed in the entablature tier of the sheet lobe SS17 near Longdi (Fig. 5a), testifying to the above mechanism having operated.

Unlike chevrons, which involve fanning columns (referred to as curvi-columnar jointing in Justus, 1978 and Lyle, 2000), *rosette jointing* involves columns that radiate 360° away from a central point, as observed in the entablature of the Bamanbor sheet lobe (Fig. 9e). Rosette jointing is common in basaltic provinces (e.g. Spry, 1962; Scheidegger, 1978; De, 1996), and a particularly large and impressive structure in the Late Cretaceous Rajahmundry Traps of southeastern India can be found in Sen & Sabale (2011). These structures require the local isotherms to have had a spherical shape (in three dimensions; circular in two dimensions), and the columns to have grown radially outwards, perpendicular to the spherical isotherms.

A common and popular interpretation of rosette jointing (including the 'war bonnet' structures of the Columbia River CFB province) has been that of filled lava tubes (e.g. Waters, 1960; Spry, 1962; Misra, 2002). However, in a lava tube that progressively shrinks towards the centre (or central axis in three dimensions) before closing, the central zone is the slowest to cool and the last to solidify. In rosette jointing (as in chevron jointing), the columns are narrowest at the convergence point or zone, and become wider (and fewer in number) outwards and eventually merge into the host lava without any break. Since joint density (and thus the number of columns) is directly proportional to both cooling rate and thermal gradient (Grossenbacher & McDuffie, 1995; Goehring & Morris, 2008), this indicates that the centre of the rosette was the coldest and fastest-cooling, and the peripheral areas the warmest and slowest-cooling, the opposite of what would be expected for a lava tube. Besides, the rosettes do not show concentric bands of vesicles, observed in progressively inward-solidifying lava tubes in young volcanic areas such as Hawaii (e.g. Keszthelyi & Self, 1998). Therefore, the columnar rosettes found in CFB sheet lobes (Fig. 14e) do not represent lava tubes (see also Greeley *et al.* 1998).

As for chevron jointing, ingress of meteoric water along cooling joints or through flow-top breccia has been suggested as a mechanism for forming rosette jointing (e.g. Long & Wood, 1986; DeGraff & Aydin, 1987; Lyle, 2000). Given so much evidence for water-enhanced solidification of the entablatures, we conclude that columnar rosettes such as that in Figure 9e are not cross-sections of lava tubes (termed *pyroducts* by Lockwood & Hazlett, 2010). Instead, we suggest, they are cross-sections of narrow, pipe-like subhorizontal *aqueducts* carrying meteoric water, or intersections of such aqueducts (Fig. 14e). The amount of meteoric water entering the top of a sheet lobe may vary considerably from area to area. This implies that the downward-growing entablature will also have lateral differences in solidification state or temperature, and it may not be laterally continuous, with zones of solidified basalt separated by molten or mushy regions. While vapourization of part of the meteoric water may cause explosions and fracturing, liquid water within the solidified basalt zones must move laterally as well as downward along the fracture pathways as more water enters from the top. Such pathways would stop at a melt pocket within the entablature and radial columns would grow outwards from that point.

The breccia-cored columnar rosettes of the Deccan Traps (Sheth *et al.* 2017a) have not been seen in the present study area, except that at one location, a metre-size patch of breccia with unclear contacts is found in the upper part of the lower colonnade (BB01) of the Bamanbor sheet lobe. The breccia-cored columnar rosettes were formed when blocks of flow-top breccia that fell in front of an advancing rubbly pāhoehoe sheet lobe were incorporated into the lobe which then inflated. The breccia blocks acted as cold inclusions causing spherical local isotherms (and radial jointing) in the cores of the sheet lobes (Sheth *et al.* 2017a). Currently these are the only such structures described in the world.

Figure 9f shows what we term *skeleton jointing* in the entablature of the Bamanbor sheet lobe. This feature is also common in Deccan sheet lobes (see e.g. fig. 5.50 of Sheth, 2018) but has not been formally described, to our knowledge. It consists of short, subhorizontal columns alongside a vertical fracture. The subhorizontal columns require the local isotherms to have been vertical, which would be the case if there was sustained flow of water along the vertical fracture, which acted as a secondary cooling surface (see Long & Wood, 1986). The columnar joints would have initiated on this surface and grown outwards into the surrounding, progressively solidifying lava. Unlike rosette jointing which forms along pipe-like, subhorizontal aqueducts, skeleton jointing indicates that subvertical planar fractures transported meteoric water into a sheet lobe. The planar vertical joint faces in the entablatures of the Talaja upper sheet lobe SS15 (Fig. 4c, d), and the Bamanbor sheet lobe (Fig. 9c), exposing hundreds of narrow subhorizontal columns in cross-section, evidently transported meteoric water in this manner.

6.b.3. Textural evidence for meteoric water-induced cooling and quenching

Petrographic observations also provide excellent evidence for meteoric water-induced cooling and quenching of the entablature of the Bamanbor sheet lobe. These are reflected in the abundant glass and the skeletal and dendritic crystal forms of the Fe–Ti oxide grains forming feathery and axiolitic growths (Fig. 12b–d). These quench features are absent in the lower colonnade of the Bamanbor sheet lobe, in which the Fe–Ti oxide grains are equant, and glass is absent (Fig. 12a).

Excellent evidence for meteoric water-induced quenching leading to high degrees of undercooling is also seen in the Chotila dyke, which in thin-section shows highly elongate-acicular and skeletal (hollow-cored to swallowtail) plagioclase crystals forming feathery to spherulitic arrangements, along with considerable amounts of interstitial glass (Fig. 13a–f). Some of the plagioclase crystals show innumerable tiny plagioclase spikes forming overgrowths (Fig. 13e), suggestive of very rapid cooling. Plagioclase crystal morphology is strongly dependent on the degree of undercooling ΔT, such that the crystals are tabular at small ΔT (~50 °C), but skeletal at ΔT ~100 °C, dendritic at ΔT ~200 °C, and spherulitic at ΔT ~400 °C (Lofgren, 1974; Corrigan, 1982; Vernon, 2018). Interaction of the magma with abundant meteoric water, a substance with a notably high heat capacity, would have caused such high degrees of undercooling.

The quench textures in the entablatures of the Saurashtra sheet lobes (with the Bamanbor lobe as an example) and the Chotila dyke imply that infiltration of meteoric water (and consequent steam convection) not only affected lava flows solidifying at the surface, but even dykes solidifying at some depth. The absence of pillow-palagonite complexes (of the kind found in the Columbia River province and elsewhere, e.g. Saemundsson, 1970; Swanson & Wright, 1981; Long & Wood, 1986; Lyle, 2000; Reidel *et al.* 2013) in our study area suggests that the meteoric waters were not displaced surface drainage which flooded the sheet lobe tops, but rainfall.

7. Conclusions

As pointed out by Sheth (2018), outcrop features of continental flood basalts (CFBs), such as vesicles and jointing patterns, are not features of academic interest alone, useful only in understanding CFB emplacement. They are also of high economic, engineering and industrial importance, considering hydrocarbon maturation by magma intrusions, flood basalt-hosted hydrocarbon and groundwater reservoirs, carbon dioxide and nuclear waste sequestration in flood basalts, economic mineralization and geothermal energy. As shown in studies of the Columbia River and North Atlantic Palaeogene CFB provinces, primary structures of CFB lava flows are also very useful in palaeoclimate interpretation: they suggest extensive interaction between meteoric waters and solidifying lava flows, and by inference a wet climate with abundant rainfall and surface drainage (Long & Wood, 1986; Lyle, 2000; Reidel *et al.* 2013). We have studied the primary structural and textural features of Deccan CFB sheet lobes and some associated dykes of the Saurashtra region. We find that these features (entablature tiers with irregular, chevron, rosette and skeleton jointing, and abundant glass and quench plagioclase and Fe–Ti oxides) require convective cooling, by extensive interaction with meteoric waters, not only for the sheet lobes solidifying on the surface but even for dykes solidifying at depth. This is good evidence for a wet palaeoclimate in western India at 65.5 Ma.

References

Aubele JC, Crumpler LS and Elston WE (1988) Vesicle zonation and vertical structure of basalt flows. *Journal of Volcanology and Geothermal Research* **35**, 349–74.

Barreto CJS, de Lima EF and Goldberg K (2017) Primary vesicles, vesicle-rich segregation structures and recognition of primary and secondary porosities in lava flows from the Paraná igneous province, southern Brazil. *Bulletin of Volcanology* **79**, 31. doi: 10.1007/s00445-017-1116-x.

Bondre NR, Duraiswami RA and Dole G (2004) Morphology and emplacement of flows from the Deccan volcanic province, India. *Bulletin of Volcanology* **66**, 29–45.

Bondre NR and Hart WK (2008) Morphological and textural diversity of the Steens Basalt lava flows, southeastern Oregon, USA: implications for emplacement style and nature of eruptive episodes. *Bulletin of Volcanology* **70**, 999–1019.

Borkar VD (1973) Fossil fishes from the inter-trappean beds of Surendranagar District, Saurashtra. *Proceedings of the Indian Academy of Sciences* **78**, 181–93.

Brown RJ, Blake S, Bondre NR, Phadnis VM and Self S (2011) 'A'ā lava flows in the Deccan volcanic province, India, and their significance for the nature of continental flood basalt eruptions. *Bulletin of Volcanology* **73**, 737–52.

Budkewitsch P and Robin P-Y (1994) Modelling the evolution of columnar joints. *Journal of Volcanology and Geothermal Research* **59**, 219–39.

Chayes F (1966) Alkaline and subalkaline basalts. *American Journal of Science* **264**, 128–45.

Corrigan GM (1982) The crystal morphology of plagioclase feldspar produced during isothermal supercooling and constant rate cooling experiments. *Mineralogical Magazine* **46**, 433–9.

Cucciniello C, Avanzinelli R, Sheth H and Casalini M (2022) Mantle and crustal contributions to the Mount Girnar alkaline plutonic complex and

the circum-Girnar mafic-silicic intrusions of Saurashtra, northwestern Deccan Traps. *Journal of Petrology* 63. doi: 10.1093/petrology/egac007.

De A (1996) Entablature structure in Deccan Trap flows: its nature and probable mode of origin. In *Deccan Basalts* (eds SS Deshmukh and KKK Nair), pp. 439–47. Nagpur: Gondwana Geological Society Special Volume no. 2.

DeGraff JM and Aydin A (1987) Surface morphology of columnar joints and its significance to mechanics and direction of joint growth. *Geological Society of America Bulletin* 99, 605–17.

DeGraff JM, Long PE and Aydin A (1989) Use of joint-growth directions and rock textures to infer thermal regimes during solidification of basaltic lava flows. *Journal of Volcanology and Geothermal Research* 38, 309–24.

Deshmukh SS (1988) Petrographic variations in compound flows of Deccan Traps and their significance. In *Deccan Flood Basalts* (ed. KV Subbarao), pp. 305–19. Bengaluru: Geological Society of India Memoir no. 10.

Duraiswami RA, Bondre NR, Dole G, Phadnis VM and Kale VS (2001) Tumuli and associated features from the western Deccan volcanic province, India. *Bulletin of Volcanology* 63, 435–42.

Duraiswami RA, Bondre NR and Managave S (2008) Morphology of rubbly pāhoehoe (simple) flows from the Deccan volcanic province: implications for style of emplacement. *Journal of Volcanology and Geothermal Research* 177, 822–36.

Duraiswami RA, Dole G and Bondre N (2003) Slabby pāhoehoe from the western Deccan volcanic province: evidence for incipient pāhoehoe-'a'ā transitions. *Journal of Volcanology and Geothermal Research* 121, 195–217.

Duraiswami RA, Gadpallu P, Shaikh TN and Cardin N (2014) Pāhoehoe-'a'ā transitions in the lava flow fields of the western Deccan Traps, India – implications for emplacement dynamics, flood basalt architecture and volcanic stratigraphy. In *Flood Basalts of Asia* (eds HC Sheth and L Vanderkluysen), pp. 146–66. *Journal of Asian Earth Sciences* 84.

Duraiswami RA, Sheth H, Gadpallu P, Youbi N and Chellai H (2020) A simple recipe for red bole formation in continental flood basalt provinces: weathering of flow-top and flow-bottom breccias. *Arabian Journal of Geosciences* 13, 953. doi: 10.1007/s12517-020-05973-9.

Ernst RE and Youbi N (2017) How Large Igneous Provinces affect global climate, sometimes cause mass extinctions, and represent natural markers in the geological record. *Palaeogeography, Palaeoclimatology, Palaeoecology* 478, 30–52.

Fedden F (1884) *The Geology of the Kathiawar Peninsula in Gujarat*. Kolkata: Geological Survey of India Memoir no. 21, pp. 73–136.

Forbes AES, Blake S and Tuffen H (2014) Entablature: fracture types and mechanisms. *Bulletin of Volcanology* 76, 820. doi: 10.1007/s00445-014-0820-z.

Goehring L and Morris SW (2008) Scaling of columnar joints in basalt. *Journal of Geophysical Research* 113, B10203. doi: 10.1029/2007JB005018.

Goff F (1996) Vesicle cylinders in vapour-differentiated basalt flows. *Journal of Volcanology and Geothermal Research* 71, 167–85.

Greeley R, Fagents SA, Harris RS, Kadel SD and Williams DA (1998) Erosion by flowing lava: field evidence. *Journal of Geophysical Research* 103, 27325–45.

Grossenbacher KA and McDuffie SM (1995) Conductive cooling of lava: columnar joint diameter and stria width as functions of cooling rate and thermal gradient. *Journal of Volcanology and Geothermal Research* 69, 95–103.

Guilbaud M-N, Self S, Thordarson T and Blake S (2005) Morphology, surface structures, and emplacement of lavas produced by Laki, A.D. 1783-84. In *Kinematics and Dynamics of Lava Flows* (eds M Manga and G Ventura), pp. 81–102. Geological Society of America Special Paper no. 396.

Harris AJL, Rowland SK, Villeneuve N and Thordarson T (2017) Pāhoehoe, 'a'ā, and block lava: an illustrated history of the nomenclature. *Bulletin of Volcanology* 79, 7. doi: 10.1007/s00445-016-1075-7.

James AVG (1920) Factors producing columnar structures in lavas and its occurrence near Melbourne, Australia. *The Journal of Geology* 28, 458–69.

Jay AE, Mac Niocaill C, Widdowson M, Self S and Turner W (2009) New palaeomagnetic data from the Mahabaleshwar Plateau, Deccan flood basalt province, India: implications for the volcanostratigraphic architecture of continental flood basalt provinces. *Journal of the Geological Society, London* 166, 13–24.

Jay AE, Marsh JS, Fluteau F and Courtillot V (2018) Emplacement of inflated pahoehoe flows in the Naude's Nek Pass, Lesotho remnant, Karoo continental flood basalt province: use of flow-lobe tumuli in understanding flood basalt emplacement. *Bulletin of Volcanology* 80, 17. doi: 10.1007/s00445-017-1189-6.

Jerram DA (2002) Volcanology and facies architecture of flood basalts. In *Volcanic Rifted Margins* (eds MA Menzies, SL Klemperer, CJ Ebinger and J Baker), pp. 119–32. Geological Society of America Special Paper no. 362.

Justus PS (1978) Origin of curvi-columnar joints in basalt cooling units by fracture-controlled quenching. *Eos (Transactions of the AGU)* 59, 379.

Kale VS, Bodas MS, Chatterjee P and Pande K (2020) Emplacement history and evolution of the Deccan volcanic province, India. *Episodes* 43, 278–99.

Kale VS, Dole G, Patil Pillai S, Chatterjee P and Bodas M (2022) Morphological types in the Deccan volcanic province, India: implications for emplacement dynamics of continental flood basalts. In *Large Igneous Provinces and Their Plumbing Systems* (eds RK Srivastava, RE Ernst, KL Buchan and M de Kock), pp. 341–96. Geological Society of London, Special Publication no. 518.

Kazanci N (2012) Geological background and three vulnerable geosites of the Kizilçahamam-Çamlidere Geopark project in Ankara, Turkey. *Geoheritage* 4, 249–61.

Keszthelyi LP and Self S (1998) Some physical requirements for the emplacement of long basaltic lava flows. *Journal of Geophysical Research* 103, 27447–64.

Keszthelyi L and Thordarson Th (2000) Rubbly pāhoehoe: a previously undescribed but widespread lava type transitional between 'a'ā and pāhoehoe. *Geological Society of America Abstracts with Programs* 32, 7.

Kilburn CRJ (2000) Lava flows and flow fields. In *Encyclopedia of Volcanoes* (eds H Sigurdsson, BF Houghton, SR McNutt, H Rymer and J Stix), pp. 291–306. New York: Academic Press.

Kilburn CRJ (2004) Fracturing as a quantitative indicator of lava flow dynamics. *Journal of Volcanology and Geothermal Research* 139, 209–24.

Krishnamurthy P (2020) The Deccan volcanic province (DVP), India: a review. *Journal of the Geological Society of India* 96, 9–35.

Lockwood JP and Hazlett RW (2010) *Volcanoes: Global Perspectives*. Chichester: Wiley-Blackwell, 541 pp.

Lofgren G (1974) An experimental study of plagioclase crystal morphology: isothermal crystallization. *American Journal of Science* 274, 243–73.

Long PE and Wood BJ (1986) Structures, textures, and cooling histories of Columbia River basalt flows. *Geological Society of America Bulletin* 97, 1144–5.

Lyle P (2000) The eruption environment of multi-tiered columnar basalt lava flows. *Journal of the Geological Society, London* 147, 714–22.

Macdonald GA (1953) Pāhoehoe, 'a'ā, and block lava. *American Journal of Science* 251, 169–91.

Marshall PE, Widdowson M and Murphy DT (2016) The giant lavas of Kalkarindji: rubbly pāhoehoe lava in an ancient continental flood basalt province. *Palaeogeography, Palaeoclimatology, Palaeoecology* 441, 22–37.

Merh SS (1995) *Geology of Gujarat*. Bengaluru: Geological Society of India, 222 pp.

Middlemost EAK (1989) Iron oxidation ratios, norms and the classification of volcanic rocks. *Chemical Geology* 77, 19–26.

Misra KS (1981) The tectonic setting of Deccan volcanics in southern Saurashtra and southern Gujarat. In *Deccan Volcanism and Related Basalt Provinces in Other Parts of the World* (eds KV Subbarao and RN Sukheswala), pp. 81–6. Bengaluru: Geological Society of India Memoir no. 3.

Misra KS (1999) Deccan volcanics in Saurashtra and Kutch, Gujarat, India. In *Deccan Volcanic Province* (ed. KV Subbarao), pp. 325–34. Bengaluru: Geological Society of India Memoir no. 43.

Misra KS (2002) Arterial system of lava tubes and channels in Deccan volcanics of western India. *Journal of the Geological Society of India* 59, 114–24.

Monteiro A, Duraiswami RA, Mittal T, Pujari S, Low U and Absar A (2021) Cooling history and emplacement dynamics within rubbly lava flows, southern Deccan Traps: insights from textural variations and crystal size distributions. *Bulletin of Volcanology* 83, 67. doi: 10.1007/s00445-021-01485-w.

Neill I, Meliksetian K, Allen MB, Navasardyan G and Kuiper K (2015) Petrogenesis of mafic collision zone magmatism: the Armenian sector of the Turkish-Iranian plateau. *Chemical Geology* **403**, 24–41.

Nichols RL (1936) Flow-units in basalt. *The Journal of Geology* **44**, 617–30.

Passey SR and Bell BR (2007) Morphologies and emplacement mechanisms of the lava flows of the Faroe Islands Basalt Group, Faroe Islands, NE Atlantic Ocean. *Bulletin of Volcanology* **70**, 139–46.

Peterson DW and Tilling RI (1980) Transition of basaltic lava from pahoehoe to aa, Kilauea volcano, Hawaii: field observations and key factors. *Journal of Volcanology and Geothermal Research* **7**, 271–93.

Philpotts AR and Dickson LA (2002) Millimeter-scale modal layering and the nature of the upper solidification zone in thick flood-basalt flows and other sheets of magma. *Journal of Structural Geology* **24**, 1171–7.

Philpotts AR and Lewis CL (1987) Pipe vesicles – an alternate model for their origin. *Geology* **14**, 971–4.

Pinkerton H and Wilson L (1994) Factors controlling the lengths of channel-fed lava flows. *Bulletin of Volcanology* **56**, 108–20.

Puffer JH and Student JJ (1992) Volcanic structures, eruptive style, and poster-uptive deformation and chemical alteration of the Watchung flood basalts, New Jersey. In *Eastern North American Mesozoic Magmatism* (eds JH Puffer and PC Ragland), pp. 261–78. Geological Society of America Special Paper no. 268.

Ramasamy SM (1995) Deformation tectonics of Deccan volcanics of southern Saurashtra, India and its relation to western extension of Narmada lineament. In *Magmatism in Diverse Tectonic Settings* (eds RK Srivastava and U Chandra), pp. 195–208. New Delhi: Oxford & IBH Publishers.

Reidel SP, Camp VE, Tolan TL and Martin BS (2013) The Columbia River flood basalt province: stratigraphy, areal extent, volume, and physical volcanology. In *The Columbia River Flood Basalt Province* (eds SP Reidel, VE Camp, ME Ross, JA Wolff, BS Martin, TL Tolan and RE Wells), pp. 1–43. Geological Society of America Special Paper no. 497.

Reidel SP, Tolan T and Camp V (2018) Columbia River flood basalt flow emplacement rates – fast, slow, or variable? In *Field Volcanology: A Tribute to the Distinguished Career of Don Swanson* (eds M Poland, M Garcia, V Camp and A Grunder), pp. 1–19. Geological Society of America Special Paper no. 538.

Rowland SK and Walker GPL (1990) Pahoehoe and aa in Hawaii: volumetric flow rate controls the lava structure. *Bulletin of Volcanology* **52**, 614–28.

Ryan MP and Sammis CG (1978) Cyclic fracture mechanisms in cooling basalt. *Geological Society of America Bulletin* **89**, 1295–308.

Saemundsson K (1970) Interglacial lava flows in the lowlands of southern Iceland and the problem of two-tiered columnar jointing. *Jökull* **20**, 62–77.

Samant B, Mohabey DM, Srivastava P and Thakre D (2014) Palynology and clay mineralogy of the Deccan volcanic associated sediments of Saurashtra, Gujarat: age and palaeoenvironments. *Journal of Earth System Science* **123**, 219–32.

Scheidegger AE (1978) The tectonic significance of joints in the Canary Islands. *Rock Mechanics* **11**, 69–85.

Schöbel S, de Wall H, Ganerød M, Pandit MK and Rolf C (2014) Magnetostratigraphy and ^{40}Ar-^{39}Ar geochronology of the Malwa Plateau region (northern Deccan Traps), central western India: significance and correlation with the main Deccan large igneous province sequences. *Journal of Asian Earth Sciences* **89**, 28–45.

Self S, Mittal T and Jay AE (2021) Thickness characteristics of pahoehoe lavas in the Deccan province, Western Ghats, India, and in continental flood basalt provinces elsewhere. *Frontiers in Earth Science* **8**, 630604. doi: 10.3389/feart.2020.630604.

Self S, Schmidt A and Mather TA (2014) Emplacement characteristics, time scales, and volcanic gas release rates of continental flood basalt eruptions on Earth. In *Volcanism, Impacts, and Mass Extinctions: Causes and Effects* (eds G Keller and AC Kerr), pp. 319–37. Geological Society of America Special Paper no. 505.

Self S, Thordarson T and Keszthelyi L (1997) Emplacement of continental flood basalt lava flows. In *Large Igneous Provinces: Continental, Oceanic, and Planetary Flood Volcanism* (eds JJ Mahoney and MF Coffin), pp. 381–410. American Geophysical Union, Geophysical Monograph vol. 100. Washington, DC, USA.

Sen B (2017) Lava flow transition in pāhoehoe-dominated lower pile of Deccan Traps from Manmad-Chandwad area, western Maharashtra. *Journal of the Geological Society of India* **89**, 281–90.

Sen B and Sabale AB (2011) Flow-types and lava emplacement history of Rajahmundry Traps, west of River Godavari, Andhra Pradesh. *Journal of the Geological Society of India* **78**, 457–67.

Sengupta P and Ray A (2006) Primary volcanic structures from a type section of Deccan Trap flows around Narsingpur-Harrai-Amarwara, central India: implications for cooling history. *Journal of Earth System Science* **115**, 631–42.

Shekhawat LS and Sharma VP (1996) Deccan basalts of Wankaner-Rajkot area, Gujarat. In *Deccan Basalts* (eds SS Deshmukh and KKK Nair), pp. 89–100. Nagpur: Gondwana Geological Society Special Volume no. 2.

Sheth H (2018) *A Photographic Atlas of Flood Basalt Volcanism*. New York: Springer International Publishing, 363 + xvi pp.

Sheth H (2020) "Pipe vesicles" in basalt: trails left by dense immiscible melt droplets sinking in a viscous basal thermal boundary layer. *Earth-Science Reviews* **201**, 103031. doi: 10.1016/j.earscirev.2019.103031.

Sheth H, Pal I, Patel V, Samant H and D'Souza J (2017a) Breccia-cored columnar rosettes in a rubbly pāhoehoe lava flow, Elephanta Island, Deccan Traps, and a model for their origin. *Geoscience Frontiers* **8**, 1299–307.

Sheth H, Samant H, Patel V and D'Souza J (2017b) The volcanic geoheritage of the Elephanta Caves, Deccan Traps, western India. *Geoheritage* **9**, 359–72.

Sheth HC, Zellmer GF, Kshirsagar PV and Cucciniello C (2013) Geochemistry of the Palitana flood basalt sequence and the eastern Saurashtra dykes, Deccan Traps: clues to petrogenesis, dyke-flow relationships, and regional lava stratigraphy. *Bulletin of Volcanology* **75**, 701. doi: 10.1007/s00445-013-0701-x.

Spry A (1962) The origin of columnar jointing, particularly in basalt flows. *Journal of the Australian Geological Society* **8**, 191–216.

Swanson DA and Wright RL (1981) The regional approach to studying the Columbia River Basalt Group. In *Deccan Volcanism and Related Basalt Provinces in Other Parts of the World* (eds KV Subbarao and RN Sukheswala), pp. 58–80. Bengaluru: Geological Society of India Memoir no. 3.

Thordarson T and Self S (1998) The Roza Member, Columbia River Basalt Group: a gigantic pāhoehoe lava flow field formed by endogenous processes? *Journal of Geophysical Research* **103**, 27411–45.

Tomkeieff SI (1940) The basalt lavas of the Giant's Causeway district of Northern Ireland. *Bulletin of Volcanology* **6**, 89–146.

Verma SP, Torres-Alvarado IS and Sotelo-Rodriguez ZT (2002) SINCLAS: standard igneous norm and volcanic rock classification system. *Computers and Geosciences* **28**, 711–15.

Vernon RH (2018) *A Practical Guide to Rock Microstructure*. 2nd edition. Cambridge: Cambridge University Press, 431 pp.

Vye-Brown C, Self S and Barry TL (2013) Architecture and emplacement of flood basalt flow fields: case studies from the Columbia River Basalt Group, NW USA. *Bulletin of Volcanology* **75**, 697. doi: 10.1007/s00445-013-0697-2.

Walker GPL (1971) Compound and simple lava flows and flood basalts. *Bulletin Volcanologique* **35**, 579–90.

Walker GPL (1987) Pipe vesicles in Hawaiian basaltic lavas: their origin and potential as palaeoslope indicators. *Geology* **14**, 84–7.

Waters AC (1960) Determining directions of flow in basalts. *American Journal of Science* **258A**, 350–66.

Wignall PB (2001) Large igneous provinces and mass extinctions. *Earth-Science Reviews* **53**, 1–33.

Williamson IT and Bell BR (1994) The Palaeocene lava field of west-central Skye, Scotland: stratigraphy, palaeogeography and structure. *Transactions of the Royal Society of Edinburgh: Earth Sciences* **85**, 39–75.

Wilson SA (2000) *Data Compilation for USGS Reference Materials Basalt BHVO2, Hawaiian Basalt*. United States Geological Survey Open File Report.